Q_β and Q_γ Components of Intramembranous Charge Movement in Frog Cut Twitch Fibers

CHIU SHUEN HUI and W. KNOX CHANDLER

From the Department of Physiology and Biophysics, Indiana University School of Medicine, Indianapolis, Indiana 46223; and Department of Cellular and Molecular Physiology, Yale University School of Medicine, New Haven, Connecticut 06510

ABSTRACT Intramembranous charge movement was measured in frog cut twitch fibers mounted in a double Vaseline-gap chamber with a TEA·Cl solution at 13–14°C in the central pool. When a fiber was depolarized from a holding potential of −90 mV to a potential near −60 mV, the current from intramembranous charge movement was outward in direction and had an early, rapid component and a late, more slowly developing component, referred to as I_β and I_γ, respectively (1979. *J. Physiol.* [*Lond.*]. 289:83–97). When the pulse to −60 mV was preceded by a 100–600-ms pulse to −40 mV, early I_β and late I_γ components were also observed, but in the inward direction. The shape of the Q_γ vs. voltage curve can be estimated with this two-pulse protocol. The first pulse to voltage V allows the amounts of Q_β and Q_γ charge in the active state to change from their respective resting levels, $Q_\beta(-90)$ and $Q_\gamma(-90)$, to new steady levels, $Q_\beta(V)$ and $Q_\gamma(V)$. A second 100–120-ms pulse, usually to −60 mV, allows the amount of Q_β charge in the active state to change from $Q_\beta(V)$ to $Q_\beta(-60)$ but is not sufficiently long for the amount of Q_γ charge to change completely from $Q_\gamma(V)$ to $Q_\gamma(-60)$. The difference between the amount of Q_γ charge at the end of the second pulse and $Q_\gamma(-60)$ is estimated from the OFF charge that is observed on repolarization to −90 mV. The OFF charge vs. voltage data were fitted, with gap corrections, with a Boltzmann distribution function plus a constant. The mean values of $\overline{V}$ (the potential at which, in the steady state, charge is distributed equally between the resting and active states) and k (the voltage dependence factor) were −59.2 mV (SEM, 1.1 mV) and 1.2 mV (SEM, 0.6 mV), respectively. The one-pulse charge vs. voltage data from the same fibers were fitted with a sum of two Boltzmann functions (1990. *J. Gen. Physiol.* 96:257–297). The mean values of $\overline{V}$ and k for the steeply voltage-dependent Boltzmann function, which is likely to be associated with the Q_γ component of charge, were −55.3 mV (SEM, 1.3 mV) and 3.3 mV (SEM, 0.6 mV), respectively, similar to the corresponding values obtained with the two-pulse protocol. These and other results are inconsistent with the three-state, two-transition model of charge movement proposed by Melzer, Schneider, Simon, and Szucs (1986. *J. Physiol.* [*Lond.*]. 373:481–511). On the other hand, the results are consistent with a model in which Q_β and Q_γ

Address reprint requests to Dr. W. Knox Chandler, Department of Cellular and Molecular Physiology, Yale University School of Medicine, 333 Cedar Street, New Haven, CT 06510-8026.

J. GEN. PHYSIOL. © The Rockefeller University Press · 0022-1295/91/09/0429/36 $2.00
Volume 98 September 1991 429–464

represent two separate species of intramembranous charge that appear to be able to move in a parallel and independent manner, at least during a voltage-clamp step that lasts no longer than a few hundred milliseconds.

INTRODUCTION

When an intact muscle fiber is depolarized from its normal resting potential, an electrical current is produced by intramembranous charge movement (Schneider and Chandler, 1973). Near or just past the mechanical threshold, this current has an early component, which decays with an approximately exponential time course, and a late component, sometimes called a "hump," which has a rather complex waveform. Adrian and Peres (1977, 1979), who first described these two components, used Q_β and Q_γ to denote the charge associated with the early and late components, respectively. In this article, the currents that arise from movements of Q_β and Q_γ charge will be called I_β and I_γ, respectively. Adrian and Peres showed that, for depolarizations to a potential between −60 and −40 mV, the voltage dependence of Q_γ is steeper than that of Q_β. Since the voltage dependence of tension (Hodgkin and Horowicz, 1960) and of Ca release from the sarcoplasmic reticulum (SR) (Baylor et al., 1979, 1983; Miledi et al., 1981; Maylie et al., 1987*a*, *b*) is also steep within this same range of potentials, it is tempting to speculate that Q_γ might play a role in the regulation of Ca release from the SR (Almers, 1978; Huang, 1982; Hui, 1983*b*; Vergara and Caputo, 1983).

Pronounced I_γ humps have been observed consistently in intact fibers. At the time that the experiments reported in this article were started (November, 1986), however, they had been observed only occasionally in cut fibers (Horowicz and Schneider, 1981*a*, *b*; Vergara and Caputo, 1983). Hui and Chandler (1990), working with cut fibers, found that a small, slowly developing I_γ hump became apparent when a fiber was depolarized to −60 to −55 mV and that this component became faster and more pronounced when the potential was made more positive. With depolarizations to −60 to −50 mV, the slow and complex time course of I_γ made it difficult to obtain a reliable estimate of the magnitude of the ON charge. Fortunately, the time course of OFF I_γ is rapid, so a reliable estimate of the magnitude of the OFF charge could be obtained. This was found to increase steeply when the potential of the pulse was varied from −60 to −50 mV, as first described by Adrian and Peres (1979) in intact fibers.

Between −80 and 0 mV, Hui and Chandler (1990) found that the relation between charge and voltage was asymmetrical, similar to that observed by Adrian and Almers (1976*b*). The charge vs. voltage data, at least in cut fibers, can be fitted significantly better with a sum of two Boltzmann functions than with a single Boltzmann function (Hui and Chandler, 1990). In the fit with a sum of two Boltzmann functions, one of the functions has a steep voltage dependence from −60 to −50 mV, with mean values $\overline{V}$ = −56.5 mV and k = 2.9 mV ($\overline{V}$ and k are defined in the Methods in association with Eq. 1). It seems likely that this Boltzmann function is associated with the Q_γ component of intramembranous charge movement.

This article describes another method to estimate the values of $\overline{V}$ and k of the Q_γ Boltzmann function. This method uses a two-pulse protocol and relies on the property that Q_γ charge moves very slowly at potentials near −60 mV. The mean

values of $\overline{V}$ and k that were obtained with this method are similar to those obtained for the Q_γ Boltzmann function in the fits with a sum of two Boltzmann functions. The two-pulse protocol also provides a way to estimate the waveform of I_γ after repolarization to the holding potential, −90 mV. At 13–14°C, the mean half-width of I_γ at −90 mV was 14.6 ms, whereas that of I_β was <3.8 ms. These and other findings are discussed in terms of whether Q_β and Q_γ are linked according to the three-state, two-transition model of charge movement proposed by Melzer et al. (1986) or whether they represent two separate species of charge that can move in a parallel and independent manner (Adrian and Huang, 1984; Huang, 1986; Huang and Peachey, 1989).

A preliminary report of some of this work has been presented to the Biophysical Society (Hui and Chandler, 1988).

METHODS

The experiments, except the one illustrated in Fig. 4 *B*, were carried out at Yale University School of Medicine from January to April, 1987. Segments of frog cut twitch fibers were mounted in a double Vaseline-gap chamber and studied with the voltage-clamp technique, as described in Chandler and Hui (1990) and Hui and Chandler (1990). A TEA·Cl solution was used in the central pool and a Cs·glutamate solution with 20 mM EGTA was used in the end pools (Table I in Chandler and Hui, 1990). The striation spacing of the fibers was 3.5–3.6 μm, the temperature of the solution in the central pool was 13–14°C, and the holding potential was −90 mV.

The methods used for data acquisition and analysis are described in Hui and Chandler (1990). Briefly, the electrical signals corresponding to V_1, V_2, and I_2 were sampled in the sequence $V_2{:}I_2{:}V_1{:}I_2{:}V_2{:}I_2{:}V_1{:}I_2$ at a frequency of 5,000 sequences per second; values from five successive sequences were averaged and stored on a disk for subsequent analysis. Traces of TEST minus CONTROL current were obtained by subtraction of the current record obtained with a CONTROL pulse from −110 to −90 mV, suitably scaled, from the current record obtained with a TEST pulse. The time course of ON intramembranous charge movement can vary considerably with pulse potential and, at voltages near the mechanical threshold, is frequently difficult to estimate because of the small amplitude and slow time course of the current (see Fig. 6 in Hui and Chandler, 1990, and Fig. 5 of this article). On the other hand, the time course of OFF intramembranous charge movement at −90 mV is rapid and shows much less variation with pulse potential, making it likely that the charge vs. voltage curve that is determined with OFF charge is more reliable than that determined with ON charge. At large depolarizations, however, the OFF charge movement is sometimes contaminated by ionic current. In this situation, it is necessary to use ON charge for the charge vs. voltage curve obtained with a one-pulse protocol (see Fig. 7 of Hui and Chandler, 1990).

In this article, except where noted, intramembranous charge movement was determined from the OFF segment at −90 mV of the TEST minus CONTROL current, as described in Hui and Chandler (1990). First, an estimate was made of the small ionic contribution to the segment of the TEST minus CONTROL current that preceded the repolarization to −90 mV; this component arises mainly from the nonlinearity of the current vs. voltage relation for Cl (Hutter and Noble, 1960). For this estimate, a sloping straight line was least-squares fitted to the last 50 ms of the current. (In Fig. 10 *A*, three of the traces of TEST minus CONTROL current were obtained with pulse durations <100 ms. For these traces, it was necessary to use a segment of the sloping straight line from a trace obtained with a longer duration pulse.) Another sloping straight line was used to estimate the ionic current after repolarization to −90

mV. This line was obtained from a least-squares fit of an exponential function plus a sloping straight line to the final segment of the TEST minus CONTROL current, from the time that the transient component had decayed to 0.25 times its peak value to 600 ms after the beginning of the repolarization. The transition from the ionic current that preceded repolarization to the OFF ionic current at −90 mV was rounded according to the normalized voltage template (Hui and Chandler, 1990). The resulting waveform was subtracted from the TEST minus CONTROL current to give the OFF component of $\Delta I_{cm}(t)$, the current attributed to intramembranous charge movement. ΔQ_{cm}, the amount of charge, was estimated from integration of $\Delta I_{cm}(t)$ during the first 600 ms of repolarization. ΔQ_{cm} was then normalized by the value of capacitance that was obtained with the CONTROL pulse, denoted by $C(-100)$.

The half-width of the OFF $\Delta I_{cm}(t)$ at −90 mV is calculated from the time that the current, soon after repolarization, reaches its half-peak value (estimated with linear interpolation) to the time, after the peak, that it has decayed to the half-peak value (usually estimated from the quadratic function that was least-squares fitted to the points between 0.45 and 0.55 times the peak value).

Charge vs. voltage curves were constructed by plotting the values of $\Delta Q_{cm}/C(-100)$ against $V_1(\infty)$, the steady-state potential in the potential-measuring end pool; the central pool was clamped to earth potential. According to Chandler and Hui (1990) and Hui and Chandler (1990), the value of V_1 is expected to be 0.96–0.99 times the membrane potential in the central-pool region next to the Vaseline seal that separates the central pool from the voltage-measuring end pool.

Throughout this article, the simplifying assumption is frequently made that charge, or its Q_β or Q_γ component, can exist in only two states, resting and active, and that, in the steady state, the amount of charge in the active state, q (per unit length of fiber), is given by the Boltzmann distribution function,

$$q = \frac{q_{max}}{1 + \exp[-(V - \overline{V})/k]} \quad (1)$$

q_{max} denotes the maximal value of q, $\overline{V}$ represents the voltage at which steady-state charge is equally distributed between resting and active states, and k is a voltage dependence factor.

Charge vs. voltage data were least-squares fitted with either a single Boltzmann function plus a constant (two-pulse protocol, Fig. 6*A*) or a sum of two Boltzmann functions (one-pulse protocol, Fig. 7*A*). In either case, the fits were made "with gap corrections," i.e., with a correction for the contributions from currents under the Vaseline seals (Hui and Chandler, 1990). With the one-pulse protocol, but not with the two-pulse protocol, each fitted curve was corrected to have a value of zero at −90 mV (the holding potential) and at −110 mV (the potential of the CONTROL pulse) by subtraction of the sloping straight line that intersected the original curve at −90 and −110 mV.

The statistical significance of a difference between two sets of results was determined with the two-tailed t test. If $P < 0.05$, the difference was considered to be significant.

RESULTS

Intramembranous Charge Movement at −60 mV from a Holding Potential of −90 mV

Fig. 1 shows an experiment that was carried out to determine whether a late I_γ current can be observed in a cut fiber, studied under our experimental conditions, when it is depolarized to a voltage near or just past the mechanical threshold. Fig. 1*A* shows $V_1(t)$ (top set of traces) and TEST minus CONTROL currents (bottom set

of traces) that were recorded with depolarizing pulses of different durations to −60 mV. The superimposed ON currents show an early, transient outward I_β component, which decayed within tens of milliseconds, followed by a more slowly decaying outward component. After repolarization, the OFF currents show an early inward component that decayed within tens of milliseconds to a nearly steady level. The amplitudes of both the transient and maintained inward OFF currents progressively increased with pulse duration.

Since the plasma membrane of frog muscle is permeable to Cl (Hodgkin and

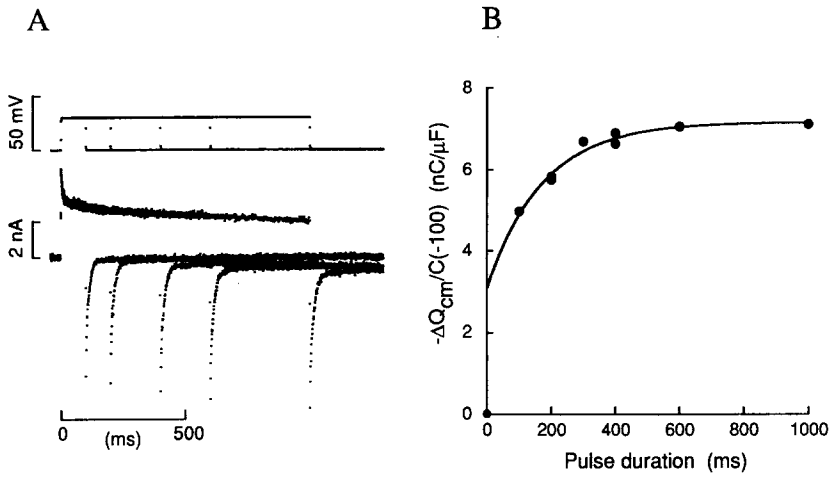

FIGURE 1. Time course of charge movement during a step depolarization to −60 mV. (*A*) The top set of superimposed traces shows $V_1(t)$ for 100-, 200-, 400-, 600-, and 1,000-ms depolarizations to −60 mV. In this and other experiments in this article, the holding potential was −90 mV. The bottom set of traces shows the corresponding TEST minus CONTROL currents. (*B*) The amount of OFF charge measured after repolarization to −90 mV (●) is plotted with reverse polarity as a function of pulse duration, from the experiment illustrated in *A*. A point has been included at the origin because the amount of OFF charge is zero without a pulse. In this and subsequent figures, measurements of charge movement (ΔQ_{cm}) have been normalized by $C(-100)$, the capacitance that was measured in the CONTROL trace when V_1 was stepped from −110 to −90 mV. The curve represents a best least-squares fit of the data, except for the point at the origin, with an exponential function plus a constant; it is given by [−4.1·exp(−*t*/171 ms) + 7.2] nC/μF. Fiber 407872; diameter, 98 μm; time after saponin treatment of the end-pool segments, 126–141 min.

Horowicz, 1959; Hutter and Noble, 1960), Cl is expected to enter the fiber during a period of depolarization. In Fig. 1 *A*, such entry probably accounts for the progressive increase in amplitude of the maintained OFF current and part of the slowly decaying outward ON current. These changes in current occur very slowly and appear to have an approximately linear time course. Hence, they are expected to be included in the estimate of ionic current and, consequently, to introduce little error into the measurement of any component of charge movement that is complete within a few tens of milliseconds after a step change in potential.

The ON records in Fig. 1 *A* clearly show an early I_β component. The late I_γ component is difficult to resolve because it has a small amplitude and slow time course. Such a component appears to be present, however, since the amount of OFF charge progressively increased with pulse duration (Fig. 1 *B*). On the assumption of ON/OFF charge equality, Fig. 1 *B* shows the time course of ON charge at times ≥ 100 ms. Although this time course is expected to be complex (Adrian and Peres, 1977, 1979; Huang, 1982; Hui, 1983*a*, *b*; Fig. 10 *A* in this article), an estimate of its duration can be obtained from a least-squares fit of an exponential function plus a constant to the points at times ≥ 100 ms. The time constant of the exponential is 171 ms, its amplitude is 4.1 nC/μF, and the value of the curve at time zero is 3.1 nC/μF. If the approximation is made that the exponential function in Fig. 1 *B* provides an adequate description of the movement of ON Q_γ charge during the entire time course of a 1,000-ms pulse to −60 mV, the contributions of Q_γ and Q_β to the total amount of charge that moved during the pulse would be equal to, respectively, the amplitude of the exponential function, 4.1 nC/μF, and the value of the curve at zero time, 3.1 nC/μF. These values are rough estimates, at best, since the ON time course of I_γ is expected to be delayed and to not follow a simple decaying exponential waveform (Adrian and Peres, 1977, 1979; Huang, 1982; Hui, 1983*a*, *b*; Fig. 10 *A* in this article).

Before the records in Fig. 1 *A* were taken, the charge vs. voltage curve was determined with single depolarizing pulses to different potentials. The charge vs. voltage data were least-squares fitted, with gap corrections, with a sum of two Boltzmann functions, as was done in Fig. 9 *B* in Hui and Chandler (1990) and in Fig. 7 *A* in this article. The Boltzmann function (Eq. 1) with the steeper voltage dependence (smaller value of k) was tentatively identified with Q_γ and the other Boltzmann function with Q_β. For Q_β, $\overline{V} = -44.8$ mV, $k = 11.0$ mV, and $q_{max}/c_m = 14.1$ nC/μF; for Q_γ, $\overline{V} = -65.3$ mV, $k = 3.0$ mV, and $q_{max}/c_m = 13.3$ nC/μF (fiber 407872 in Table III in Hui and Chandler, 1990). According to this fit, with gap corrections, the steady-state difference between the amounts of charge in the active state at $V_1 = -60$ mV and $V_1 = -90$ mV is 2.3 nC/μF for Q_β and 8.4 nC/μF for Q_γ. These values are in rough agreement with the values 3.1 and 4.1 nC/μF, respectively, that were obtained from the exponential fit in Fig. 1 *B* and given in the preceding paragraph.

The main conclusion from the experiment illustrated in Fig. 1 is that, during a step to −60 mV from a holding potential of −90 mV, charge movement consists of an early I_β component and a late I_γ component.

Charge Movement from 200 to 1,200 ms at Potentials between −70 and −50 mV

In intact fibers at 2–7°C, movements of Q_γ charge that require > 100 ms to complete are normally observed only in a narrow range of potentials near or just beyond the mechanical threshold (Adrian and Peres, 1977, 1979; Huang, 1982; Hui, 1983*a*, *b*). To explore these slow kinetics further, the amount of Q_γ charge that failed to reach a steady-state level after a 200-ms pulse was estimated from the difference between the values of OFF charge after 200- and 1,200-ms pulses. Fig. 2 shows this difference plotted as a function of pulse potential. In this fiber, the largest difference was observed at −60 mV where the OFF charge after the 1,200-ms pulse was 1.1 nC/μF larger, in absolute value, than that after the 200-ms pulse. For potentials ≤ -66 mV

and ≥ -54 mV, any difference was too small to be resolved reliably. In other experiments, the I_γ hump was complete within 100 ms or less after depolarizations to potentials ≥ -50 mV (Figs. 5 and 10*A*).

The conclusion from this experiment is that, at 13–14°C, pulses that last at least 200 ms should be used to measure steady-state changes in charge near −60 mV. With 200-ms pulses the maximal error is expected to be ~1 nC/μF (Fig. 2), and with 400-ms pulses the maximal error is expected to be reduced to ~0.4 nC/μF (Fig. 1*B*).

Charge Movement at −60 mV after a Prepulse to −40 mV

Fig. 3 shows traces obtained with a two-pulse protocol that is complementary to the one-pulse protocol used in Fig. 1: each depolarization to −60 mV was preceded by a

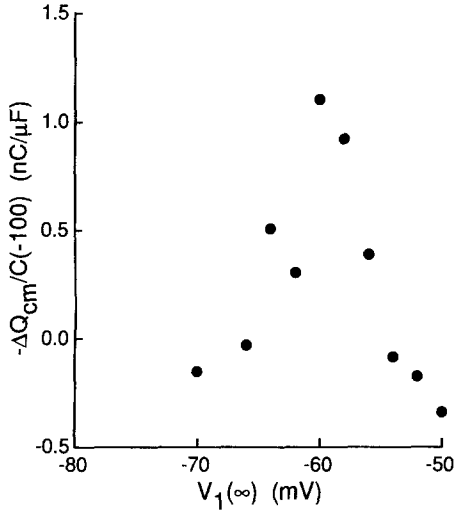

FIGURE 2. Differences between the amounts of OFF charge after 200- and 1,200-ms pulses to potentials between −70 and −50 mV. At each potential, the amount of OFF charge was measured first after a 200-ms pulse, then after a 1,200-ms pulse, and finally after a 200-ms pulse. Each filled circle gives the difference between the value obtained after the 1,200-ms pulse and the average value obtained after the 200-ms pulse. The points are plotted with reverse polarity so that a point above 0.0 corresponds to more OFF charge, in absolute value, after the 1,200-ms pulse than after the 200-ms pulse. The estimates of charge difference shown in this figure are likely to be more accurate than the individual estimates of OFF charge shown in other figures in this article. Fiber 331871; diameter, 117 μm; time after saponin treatment of the end-pool segments, 145–170 min.

200-ms prepulse to −40 mV. Fig. 3*A* shows $V_1(t)$ (top set of traces) and TEST minus CONTROL currents (bottom set of traces) from the fiber that was used for Fig. 1. During the pulse to −40 mV, there was an outward current that consisted of an early transient component that decayed within tens of milliseconds to an approximately steady level. During this period, the amounts of Q_β and Q_γ charge in the active state are expected to reach steady-state values appropriate for −40 mV. On repolarization to −60 mV, these amounts are expected to decrease and, if the pulse is sufficiently long, to reach new steady-state values. During this period at −60 mV, the current consisted of an early transient inward component followed by a slowly changing component. The time course of the slow component is difficult to resolve but can be estimated, on the assumption of ON/OFF charge equality, from measurements of OFF charge obtained after repolarization to −90 mV.

Fig. 3 *B* shows the values of OFF charge at −90 mV plotted as a function of the duration of the pulse to −60 mV, from the experiment illustrated in Fig. 3 *A*. The amount of charge progressively decreased with increasing pulse duration and reached an approximately steady level of ~8.3 nC/μF by 600–1,000 ms. After the first 100 ms, the duration of the shortest pulse at −60 mV, this decrease approximately followed an exponential time course, which is shown by the continuous curve. The time constant of the exponential function is 168 ms, its amplitude is 4.3 nC/μF, and the value of the curve at zero time is 12.6 nC/μF.

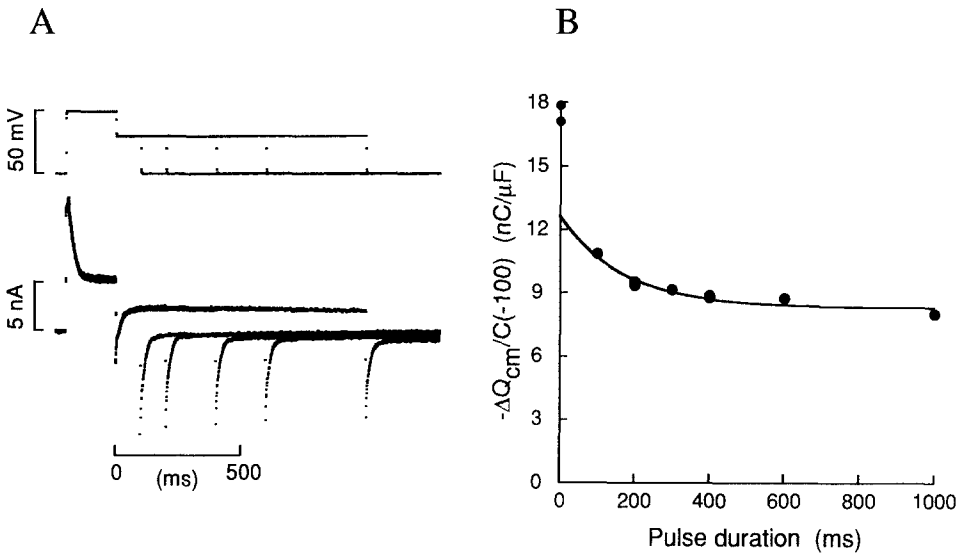

FIGURE 3. Time course of charge movement during a depolarization to −60 mV that was preceded by a 200-ms depolarization to −40 mV. (*A*) The top set of superimposed traces shows $V_1(t)$ for 100-, 200-, 400-, 600-, and 1,000-ms depolarizations to −60 mV. The bottom set of traces shows the corresponding TEST minus CONTROL currents. (*B*) The filled circles show the amount of OFF charge that was measured after repolarization to −90 mV. They are plotted with reverse polarity as a function of the duration of the −60-mV pulse, from the experiment illustrated in *A*. The two points associated with zero pulse duration (mean value, 17.5 nC/μF) were obtained when the fiber was repolarized to −90 mV immediately after the prepulse to −40 mV; these points were obtained at the beginning and end of the experiment illustrated in *A*. The curve represents a best least-squares fit of the data, except for the points at time zero, with an exponential function plus a constant; it is given by [4.3·exp (−*t*/168 ms) + 8.3] nC/μF. Same fiber as in Fig. 1; time after saponin treatment of the end-pool segments, 125–140 min.

In Fig. 1, when the voltage was stepped from −90 to −60 mV, the fast and slow components of charge movement were identified with Q_β and Q_γ, respectively, following Adrian and Peres (1979). When the pulse to −60 mV is preceded by a −40-mV prepulse (Fig. 3), it seems reasonable to make the same tentative identification of the fast and slow components of charge movement. If the approximation is made that the exponential function in Fig. 3 *B* adequately describes the movement of

Q_γ charge during the entire time course of the 1,000-ms pulse to −60 mV, the contributions of Q_γ and Q_β to the total amount of charge that moved during the pulse would be equal, respectively, to the amplitude of the exponential function, 4.3 nC/μF, and to the difference between the mean value of the two points at zero time (17.5 nC/μF) and the exponential curve at zero time (12.6 nC/μF), 4.9 nC/μF. These values should be taken as rough approximations, however, since it is not known whether, after a −40-mV prepulse, the time course of I_γ at −60 mV is exponential. Indeed, at −90 mV the time course of I_γ appears to be nonexponential (Fig. 9 *B*).

As mentioned in the description of Fig. 1 *B*, the charge vs. voltage data from the fiber used in Figs. 1 and 3 were fitted with a sum of two Boltzmann functions, with gap corrections. According to the fit, the steady-state difference between the amounts of charge in the active state at $V_1 = -40$ mV and $V_1 = -60$ mV is 4.8 nC/μF for Q_β and 1.4 nC/μF for Q_γ. The value for Q_β, 4.8 nC/μF, is in good agreement with the estimate of 4.9 nC/μF from the exponential fit in Fig. 3 *B* (preceding paragraph). On the other hand, the value for Q_γ, 1.4 nC/μF, is considerably smaller than the estimate from Fig. 3 *B*, 4.3 nC/μF. Other experiments gave better agreement between the two estimates of Q_γ and these results will be described below in connection with Table I.

After a 1,000-ms pulse to −60 mV, a slightly smaller value of OFF charge was measured in Fig. 1 *B* (7.1 nC/μF) than in Fig. 3 *B* (8.0 nC/μF). The difference, 0.9 nC/μF, may be genuine since the two measurements were made ~1 min apart. For each duration of the −60-mV pulse, successive measurements were made with (Fig. 3) and without (Fig. 1) the −40-mV prepulse. 13 such paired measurements were made on eight fibers in which a 1,000–1,300-ms pulse to −60 mV was used. On average, the absolute values of OFF charge were larger, by 0.29 nC/μF (SEM, 0.12 nC/μF), when a −40-mV prepulse was used; the difference is significantly different from zero.

This small difference may be due to a very slow, small component of charge movement that occurs at −60 mV after a prepulse to −40 mV. In Fig. 3 *B*, the point at 600 ms lies above the theoretical curve and the point at 1,000 ms lies below it; the difference between the values of these points is 0.72 nC/μF, whereas the difference between the values of the theoretical curve at 600 and 1,000 ms is only 0.11 nC/μF. In seven experiments of this type, the experimental points at 1,000–1,200 ms always lay below the corresponding fitted exponential curves and, in six of the experiments, the points at 500–800 ms lay above the corresponding curves. This suggests that, after a prepulse to −40 mV, the distribution of Q_γ charge at −60 mV does not completely reach a steady state within 1,000 ms.

Fig. 4 *A* shows an attempt to resolve, directly, the slow I_γ current at −60 mV after a prepulse to −40 mV. The top trace shows the voltage associated with a 1,000-ms pulse to −60 mV, from Fig. 3 *A*. The bottom noisy trace shows the corresponding current from Fig. 3 *A*, plotted at 10 times the gain. The points during the −40-mV prepulse and during the first 10 ms of the −60-mV pulse are off scale. Thereafter, the current at −60 mV had a rapidly decaying component (identified with I_β), a small slowly decaying component (identified with I_γ), and a component with a negative slope (considered to be ionic), which is best resolved at late times.

Although the current record in Fig. 4 *A* is very noisy, an attempt was made to separate the segment at −60 mV into I_β and I_γ components. For this purpose, the current was least-squares fitted, after the first 5 ms, with a sum of two exponential

functions plus a sloping straight line. Within the noise of the record, the fit (not shown) was good and, as a rough approximation, the two exponential functions, with time constants 18 and 164 ms, were identified with I_β and I_γ, respectively. The two curves in Fig. 4 *A* show the sloping straight line alone (considered to be the ionic current) and the sloping straight line plus the exponential function with the 164-ms

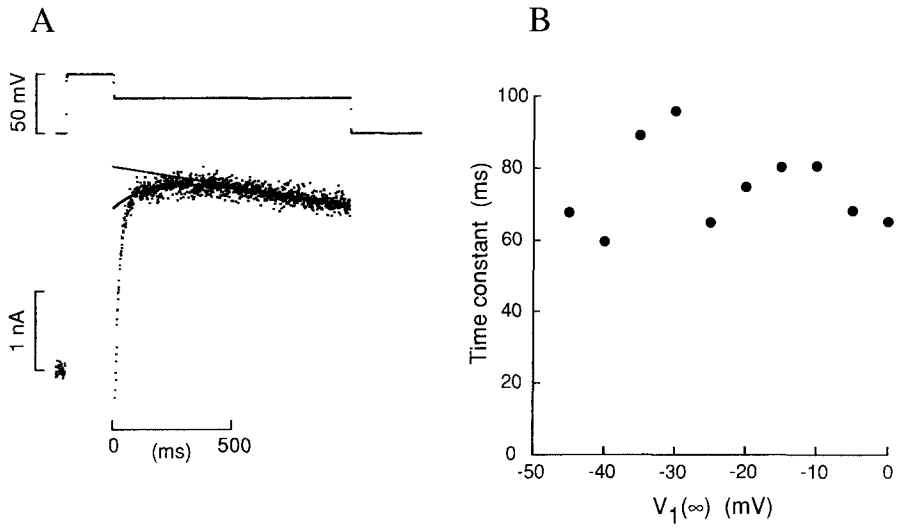

FIGURE 4. A slow component of charge movement at −60 mV after a 200-ms conditioning depolarization to −40 mV. (*A*) The top trace shows $V_1(t)$ and the bottom trace shows the corresponding TEST minus CONTROL current plotted at high gain; the points during the prepulse and during the first 10 ms of the −60-mV pulse are off scale. The current trace at −60 mV, after the first 5 ms, was least-squares fitted by a sum of two exponential functions plus a sloping straight line. The two continuous curves in the figure show the sloping straight line alone and the sloping straight line plus the exponential function with the larger time constant, 164 ms. This exponential function accounts for 5.8 nC/μF of the total charge, 11.5 nC/μC. The time constant of the other exponential function (not shown) was 18 ms. The same traces as shown for the 1,000-ms pulse to −60 mV in Fig. 3 *A*. (*B*) In a different experiment, a 784-ms pulse to −55 mV was preceded by a prepulse to different potentials. The duration of the prepulse was 200 ms with prepulse potentials −45 to −20 mV and 100 ms with prepulse potentials −15 to 0 mV. The current trace at −55 mV, after the first 5 ms, was least-squares fitted by a sum of two exponential functions plus a sloping straight line, as was done in *A*. The filled circles show the time constant of the exponential function with the larger time constant plotted as a function of prepulse potential. Fiber 920891 (studied by C. S. Hui and W. Chen at the Indiana University School of Medicine); diameter, 124 μm; time after saponin treatment of the end-pool segments, 152–169 min.

time constant. The amount of charge associated with this exponential function is 5.8 nC/μF. These estimates of the time constant and amount of Q_γ charge are considered to be approximate, however, because the amplitude of the I_γ exponential function is similar to that of the noise in the current record and, as mentioned above, the time course of I_γ may not be exponential.

The fiber used for Figs. 1, 3, and 4 *A* was selected because it was the only fiber in which charge movement was measured at −60 mV both from the holding potential and after a prepulse to −40 mV. This fiber was somewhat unusual in that the two estimates of the I_γ time constant were similar, 168 ms in Fig. 3 *B* and 164 ms in Fig. 4 *A*. In other fibers, the methods illustrated in Figs. 3 *B* and 4 *A* gave different values, as will now be described.

Table I gives information about movements of Q_γ charge at −60 mV, after a prepulse to −40 mV, in 10 fibers. Columns 3 and 4 give the values of τ_β and τ_γ, respectively, that were estimated with the two-exponential fitting procedure illustrated in Fig. 4 *A*. The mean values of τ_β and τ_γ were 12 and 88 ms, respectively. Column 5 gives the estimates of Q_γ, as given by the amount of charge associated with the τ_γ exponential function.

Columns 6 and 7 of Table I give the estimates of τ_γ and Q_γ obtained from the measurements of OFF charge, as illustrated in Fig. 3. The mean values of Q_γ in columns 5 and 7 are similar, perhaps fortuitously, and the difference, even when calculated pairwise, is not significant.

On the other hand, the mean values of τ_γ in columns 4 and 6 of Table I are different, significantly, by a factor of 2.7. If this difference is genuine, it might arise from a nonexponential time course of I_γ at −60 mV, as mentioned above. In this case, the estimates in column 4 would depend mainly on the first 100 ms of the current, whereas those in column 6 would depend mainly on the current at times ≥ 100 ms. On the other hand, the difference might arise from difficulties in the resolution of I_γ at −60 mV; the small amplitude and slow time course of I_γ might contribute different errors in the two methods used to estimate τ_γ.

In seven of the fibers used for Table I, charge vs. voltage data were obtained with the usual one-pulse protocol and fitted, with gap corrections, with a sum of two Boltzmann distribution functions. The parameters from the fits are given in Table III in Hui and Chandler (1990). Column 8 of Table I gives the differences in the steady-state amounts of charge in the active state that were calculated from the Q_γ Boltzmann functions at $V_1 = -60$ mV and $V_1 = -40$ mV. These values are similar to those in columns 5 and 7 and the differences, even when calculated pairwise, are not significant.

The main conclusions from the experiments illustrated in Figs. 1–4 *A* and Table I are that (*a*) the Q_γ component of intramembranous charge moves slowly when the potential is stepped from −90 to −60 mV (Fig. 1) or from −90 mV to a potential within ~5 mV of −60 mV (Fig. 2), (*b*) Q_γ charge also moves slowly when the potential is stepped from −40 to −60 mV (Figs. 3 and 4 *A*; Table I), and (*c*) these movements of Q_γ charge require several hundred milliseconds to complete at 13–14°C. Unfortunately, it is difficult to determine the exact time course of I_γ at −60 mV because of the current's small amplitude and slow kinetics.

Finding (*a*) confirms results on intact fibers from several laboratories (Adrian and Peres, 1977, 1979; Huang, 1982; Hui 1983*a*, *b*). On the other hand, finding (*b*) is different from the results in intact fibers reported by Huang (1984). He found that the time course of the OFF I_γ was always rapid, even at potentials where the ON I_γ was delayed and prolonged. Although the reason for the difference between his results and ours has not been established, a possible explanation is that a small,

TABLE I

Apparent Time Constant and Amount of Q_γ Charge That Moves at −60 mV after a Prepulse to −40 mV

(1)	(2)	(3)	(4)	(5)	(6)	(7)	(8)
Fiber reference	Time after saponin treatment	From the current at −60 mV			From OFF currents at −90 mV		From fit with two Boltzmann functions
		τ_β	τ_γ	Q_γ	τ_γ	Q_γ	Q_γ
	min	*ms*	*ms*	*nC/μF*	*ms*	*nC/μF*	*nC/μF*
117871	82–92	7	68	4.5	530	5.6	—
120871	103–108 (63–113)	8	37	8.2	120	4.1	6.4
126871	80–91	17	99	6.0	140	6.8	—
331871	181 (119–128)	14	107	6.3	—	—	8.3
401872	98 (67–91)	9	69	3.1	—	—	6.4
407871	58–72 (77–122)	11	93	4.1	285	4.2	5.8
407872	125–140 (54–104)	18	164	5.8	168	4.3	1.4
408871	58	11	96	2.9	—	—	—
409871	80–92 (101–146)	10	72	5.9	218	6.2	10.2
	168–176 (101–146)	15	91	6.9	184	4.8	10.2
409872	93 (56–82)	9	70	8.5	—	—	9.6
Mean		12	88	5.7	235	5.1	7.3
SEM		1	10	0.6	53	0.4	1.1

Column 1 gives the fiber references. Column 2 gives the times that elapsed from the saponin treatment of the end-pool segments to the measurements; the times not in parentheses refer to the measurements used for columns 3–7 and the times in parentheses refer to the measurements used for column 8. The values in columns 3–5 were obtained from the current that was measured during a 800–1,200-ms pulse to −60 mV. Each pulse was preceded by a 200-ms prepulse to −40 mV (except for fiber 117871 in which a 100-ms prepulse was used). A sum of two exponential functions plus a sloping straight line was least-squares fitted to each TEST minus CONTROL current at −60 mV, after the first 5 ms (see Fig. 4 *A*). The smaller time constant from the fit is denoted by τ_β (column 3) and the larger time constant by τ_γ (column 4). The charge associated with the τ_γ exponential function is denoted by Q_γ (column 5). The values in columns 3–5 represent mean values from one to three records. The values in columns 6 and 7 were obtained from two-pulse experiments similar to those used for columns 3–5 except that the duration of the pulse to −60 mV was varied from 80 to 1,200 ms. The relation between the amount of OFF charge that moved after repolarization to −90 mV and the duration of the −60-mV pulse was least-squares fitted by an exponential function plus a constant (as illustrated in Fig. 3 *B*). Columns 6 and 7 give, respectively, the values of the time constant of the exponential function and of the charge associated with it, as determined from the fitted scaling constant of the exponential function. Column 8 gives the differences in the amounts of steady-state Q_γ charge in the active state at V_1 = −60 mV and V_1 = −40 mV, with gap corrections; each value was estimated from the Q_γ Boltzmann function that was obtained from a least-square fit, with gap corrections, of a sum of two Boltzmann functions to charge vs. voltage data from a one-pulse experiment (Table III of Hui and Chandler, 1990). Fiber diameters, 93–117 μm.

prolonged I_γ might have been obscured in Huang's estimates of current by noise from the microelectrodes used in the three-microelectrode method for the measurement of current.

To explain his findings, Huang (1984) proposed a simple two-state model in which charge can exist in either a resting or an active state. The forward and backward rate constants for the movement of charge between the two states depend both on potential and on the amount of charge that is in the active state. At any given voltage,

the forward and backward rate constants increase as the amount of charge in the active state increases. If a fully polarized fiber, with little charge in the active state, is depolarized past the mechanical threshold, the movement of charge from the resting to the active state is initially very slow and later becomes rapid as the amount of charge in the active state increases. Under certain conditions, Huang showed that the time course of charge movement calculated with his model can show humps similar to those associated with I_γ. After repolarization from a depolarized state in which a significant amount of charge is in the active state, Huang showed that the rearrangement of charge is expected to be relatively rapid at all potentials, including those near the mechanical threshold. In Huang's model, both the forward and backward rate constants increase by the same proportion when the amount of charge in the active state increases. Consequently, their ratio does not change and the steady-state distribution of charge between resting and active states satisfies a Boltzmann distribution function.

Thus, Huang's model predicts a steady-state charge vs. voltage curve that satisfies a Boltzmann distribution function, the presence of humps in the time course of ON charge movement at certain potentials, and a rapid, monotonically decaying time course of OFF charge movement. Unfortunately, the model, at least in its original form, predicts a rapid time course of OFF charge movement at −60 mV and this is inconsistent with finding (*b*) of our observations.

Effect of Prepulse Potential on τ_γ *at* -55 *mV*

Fig. 4 *B* shows the values of τ_γ plotted as a function of prepulse potential. In this experiment, τ_γ was estimated with the two-exponential fitting procedure illustrated in Fig. 4 *A*; the potential of the second pulse was −55 mV. The data show scatter but no consistent variation with prepulse potential. Hence, within the accuracy of the measurements, the potential of the prepulse has little consistent effect on the time course of the decay of I_γ at −55 mV after a more depolarizing prepulse.

Charge Movement Studied with a Two-Pulse Protocol

According to the experiments illustrated in Figs. 1–4 and Table I, after a voltage step to −60 mV at 13–14°C, Q_β charge is expected to move sufficiently rapidly that a steady state is reached after 50–100 ms, whereas the movement of Q_γ charge is expected to require several hundred milliseconds to complete. This difference in the kinetics of Q_β and Q_γ at −60 mV can be used to design a two-pulse protocol to estimate the shape, but not the amplitude, of the steady-state charge vs. voltage curve of Q_γ. A 100–600-ms pulse to voltage V causes the amounts of Q_β and Q_γ charge in the active state to reach new steady-state levels $Q_\beta(V)$ and $Q_\gamma(V)$, respectively, as was done in the experiment illustrated in Fig. 3 *A*, in which a pulse to −40 mV was used. This pulse is typically followed by a 100-ms pulse to −60 mV. The second pulse is sufficiently long to allow the amount of Q_β charge in the active state to reach $Q_\beta(-60)$ but is too short to allow the amount of Q_γ charge to reach $Q_\gamma(-60)$. At the end of the pulse, the amount of Q_γ charge in the active state is equal to $Q_\gamma(-60) + \rho[Q_\gamma(V) - Q_\gamma(-60)]$, in which ρ is less than unity. The value of ρ depends on the kinetics associated with the movement of Q_γ charge at −60 mV; for example, if the time course of I_γ were given by a decreasing exponential function with a time

constant τ_γ (in milliseconds), ρ would equal exp $(-100/\tau_\gamma)$. On repolarization to -90 mV, the amount of OFF charge, Q_{OFF}, is given by

$$Q_{OFF} = Q_\beta(-60) - Q_\beta(-90) + Q_\gamma(-60) + \rho[Q_\gamma(V) - Q_\gamma(-60)] - Q_\gamma(-90) \quad (2)$$

$$= [Q_\beta(-60) - Q_\beta(-90) + (1 - \rho)Q_\gamma(-60) - Q_\gamma(-90)] + \rho Q_\gamma(V) \quad (3)$$

The term in brackets on the right-hand side of Eq. 3 depends on ρ and on the steady-state levels of Q_β and Q_γ charge at -60 and -90 mV. If the value of ρ does not depend on V, as suggested by the results in Fig. 4 *B*, the term in brackets is independent of V. In this case, Q_{OFF} is equal to a constant plus a term that is proportional to $Q_\gamma(V)$. Consequently, the voltage-dependent component of Q_{OFF} gives the voltage dependence of Q_γ.

Fig. 5 *A* shows traces obtained with the two-pulse protocol just described. The top trace shows a record of $V_1(t)$ in which a 400-ms pulse to -40 mV was followed by a 100-ms pulse to -62 mV. The other traces show TEST minus CONTROL currents. The potential of the first pulse was varied, as indicated, whereas the potential of the second pulse was always -62 mV. In the first two current traces, the ON current shows an early transient component that is typical of I_β. In the next trace, at -50 mV, this early component was followed by a prominent I_γ hump that became earlier and briefer when the potential was made more positive. Although a small I_γ hump may also be present in the -60-mV trace, it cannot be resolved reliably, as described in connection with Fig. 1. In the bottom trace, at 0 mV, the ON current shows a slowly developing inward component, possibly carried by Ca (Horowicz and Schneider, 1981*a*).

In Fig. 5 *A*, all the OFF currents at -90 mV decayed rapidly.

OFF Charge vs. Voltage Curves in a Two-Pulse Experiment

Fig. 6 *A* shows the values of OFF charge at -90 mV plotted as a function of the potential of the first pulse, from the experiment illustrated in Fig. 5 *A*. According to Eq. 3, if ρ is independent of V, the OFF charge vs. voltage data should be given by a constant plus ρ times $Q_\gamma(V)$. The curve in Fig. 6 *A* shows the least-squares fit, with gap corrections (see Methods), of a constant plus a Boltzmann function for $Q_\gamma(V)$, with $\overline{V} = -57.2$ mV and $k = 1.4$ mV. Only the filled circles, which were obtained between $V_1 = -90$ and -30 mV, were used for the fit. The open circles, which were obtained between $V_1 = -20$ and 0 mV, lie above the curve.

The general features shown by the data in Fig. 6 *A* were found in five similar experiments. In each experiment, between $V_1 = -90$ mV and -40 to -20 mV (the exact potential depended on the fiber), the values of OFF charge showed a sigmoid dependence on V_1. Between $V_1 = -90$ and about -65 mV, the value of OFF charge was approximately constant. As V_1 was increased from about -60 to -50 mV, the value of OFF charge abruptly increased and then was approximately constant for an interval of at least 20 mV. Over this voltage range, the data were well fitted by a Boltzmann function plus a constant. At more positive potentials, the value of OFF charge increased somewhat and deviated from the Boltzmann curve. Possible reasons for this deviation will be given in the Discussion. The values of $\overline{V}$, k, and q_{max}/c_m from

the five experiments are given in columns 2–4 of Table II. The mean values are −59.2 mV, 1.2 mV, and 4.1 nC/μF, respectively.

The Voltage Dependence of the Half-Width of OFF Charge Movement in a Two-Pulse Experiment

The filled circles in Fig. 6 *B* show the values of the half-width of OFF charge movement at −90 mV, which is used as a measure of the duration of the current,

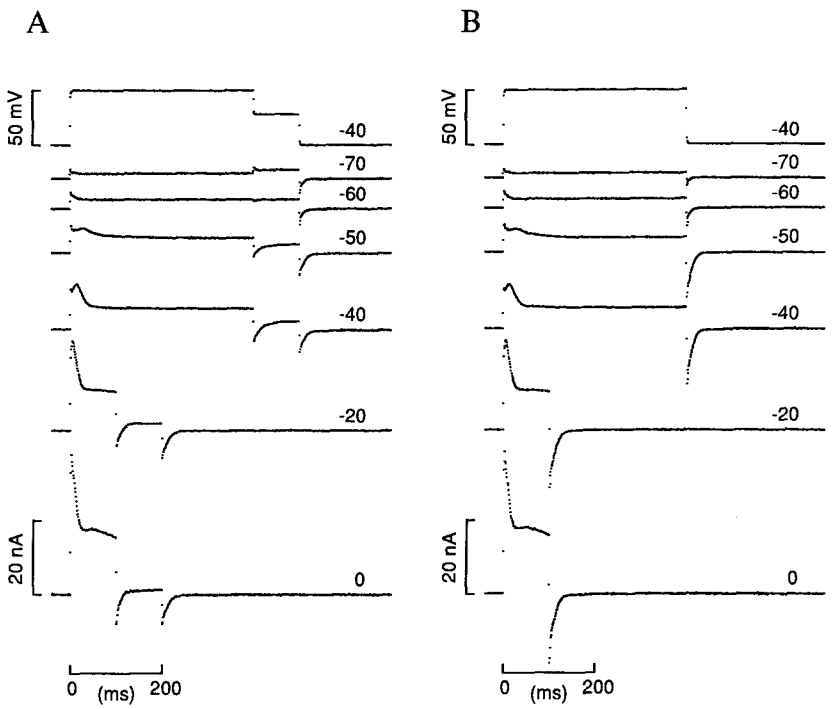

FIGURE 5. TEST minus CONTROL currents obtained with a two-pulse protocol (*A*) and a one-pulse protocol (*B*). (*A*) The top $V_1(t)$ trace was obtained with a 400-ms depolarization to −40 mV followed by a 100-ms pulse to −62 mV. The other traces show TEST minus CONTROL currents obtained with different voltages of the first pulse (indicated in millivolts). The duration of the first pulse was 400 ms for the top four current traces and 100 ms for the bottom two traces. (*B*) Same protocol as in *A* except that a second pulse was not used. Fiber 410871; diameter, 88 μm; time after saponin treatment of the end-pool segments, 50–70 min.

plotted as a function of the potential of the first pulse. Between −90 and −60 mV, the half-width was relatively constant at ~3 ms. As the potential was increased from −60 to −50 mV, the half-width increased to ~8 ms. Between −50 and 0 mV it underwent little consistent change.

Since the abrupt increase in half-width between −60 and −50 mV in Fig. 6 *B* is similar to the increase in charge in Fig. 6 *A*, it was of interest to compare the relative positions on the voltage axis of the half-width curve in Fig. 6 *B* and the Q_γ curve in

Fig. 6 *A*. To do this, an estimate was made of the voltage, $V_{1/2}$, at which the half-width would be 5.6 ms, the value midway between the mean value from −90 to −70 mV, 3.1 ms (plotted as a dashed horizontal line between −90 and −70 mV), and the mean value from −45 to 0 mV, 8.1 ms (plotted as a dashed horizontal line between −45

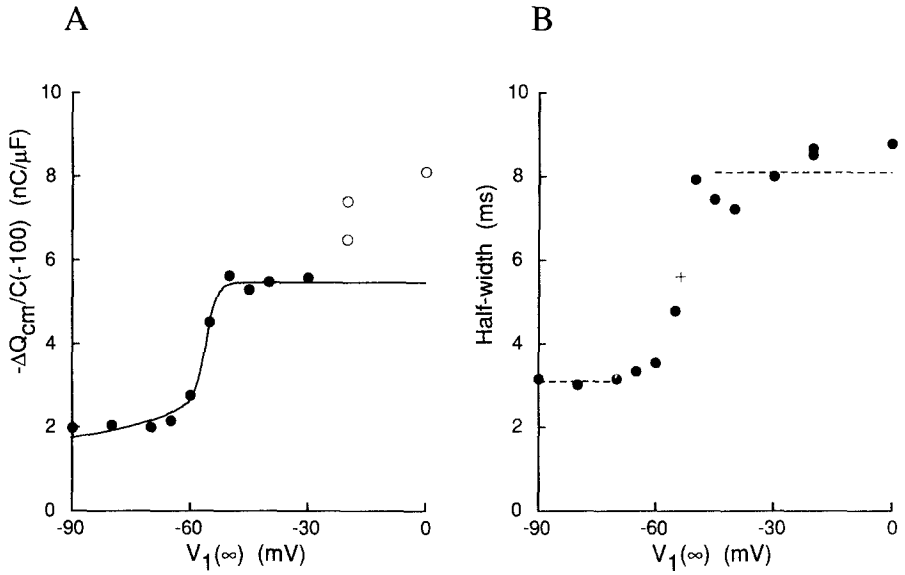

FIGURE 6. Properties of OFF charge movement at −90 mV in a two-pulse experiment, from the experiment in Fig. 5 *A*. (*A*) The filled and open circles show the values of OFF charge plotted, with reverse polarity, as a function of the potential of the first pulse. The continuous curve shows the least-squares fit, with gap corrections, of a single Boltzmann function plus a constant to the filled circles; the open circles were not used for the fit. The parameters of the Boltzmann function are $\overline{V}$ = −57.2 mV, k = 1.4 mV, and q_{max}/c_m = 3.9 nC/μF; the value of the constant is 1.1 nC/μF. The small progressive increase in the value of the theoretical curve between −90 and −65 mV arises from charge movement under the Vaseline seals (see Figs. 2–5 in Hui and Chandler, 1990). (*B*) The filled circles show the half-widths of the current carried by OFF charge movement at −90 mV, plotted as a function of the potential of the first pulse. The lower horizontal dashed line shows the mean value of half-width between −90 and −70 mV, 3.1 ms; the upper horizontal dashed line shows the mean value between −45 and 0 mV, 8.1 ms. The cross is plotted with the abscissa equal to $V_{1/2}$, −53.7 mV, and the ordinate equal to the average value of the two horizontal lines, 5.6 ms. The value of −53.7 mV in the voltage-measuring end pool corresponds to a value of −54.9 mV for the mean membrane potential in the central-pool region (based on a linear gradient of potential along the inside of the fiber and $r_e/(r_i + r_e)$ = 0.988; Hui and Chandler, 1990). Time after saponin treatment of the end-pool segments, 47–72 min.

and 0 mV). $V_{1/2}$ was estimated to be −53.7 mV by linear interpolation between the two points at −55 and −50 mV. The cross in Fig. 6 *B* marks the point where $V_{1/2}$ = −53.7 mV and the half-width = 5.6 ms. A value of −53.7 mV for the voltage in the voltage-measuring end pool corresponds to a value of −54.9 mV for the mean

membrane potential in the central-pool region where most of the measured charge movement takes place (the estimate of −54.9 mV is based on a linear gradient of potential along the inside of the fiber and $r_e/(r_i + r_e) = 0.988$; Chandler and Hui, 1990). The value of −54.9 mV is similar to −57.2 mV, the value of $\overline{V}$ for the Boltzmann curve in Fig. 6 *A*. This similarity suggests that the steeply voltage-dependent increase in half-width from −60 to −50 mV in Fig. 6 *B* is correlated with the steeply voltage-dependent Q_γ charge in Fig. 6 *A*, and that the time course of I_γ at −90 mV is longer than that of I_β.

TABLE II

Boltzmann Function Parameters for Q_γ *Obtained from Charge vs. Voltage Data*

(1)	(2)	(3)	(4)	(5)	(6)	(7)	(8)	(9)	(10)	(11)
Fiber reference	Q_γ from a two-pulse experiment			Q_γ from a one-pulse experiment			$\Delta\overline{V}$	Δk	ρ	τ_γ
	$\overline{V}$	k	q_{max}/c_m	$\overline{V}$	k	q_{max}/c_m				
	mV	*mV*	*nC/μF*	*mV*	*mV*	*nC/μF*	*mV*	*mV*		*ms*
127872	−59.4	0.2	2.6	−51.9	4.7	20.1	−7.5	−4.5	0.13	59
407871	−62.4	3.2	3.9	−58.8	3.8	12.4	−3.6	−0.6	0.31	85
409871	−60.7	1.3	4.0	−52.9	4.2	16.1	−7.8	−2.9	0.25	72
409872	−56.4	0.0	6.1	−56.5	1.6	14.5	0.1	−1.6	0.42	115
410871	−57.2	1.4	3.9	−56.5	2.3	12.6	−0.7	−0.9	0.31	85
Mean	−59.2	1.2	4.1	−55.3	3.3	15.1	−3.9	−2.1	0.28	83
SEM	1.1	0.6	0.6	1.3	0.6	1.4	1.7	0.7	0.05	9

Column 1 gives the fiber references. Columns 2–4 give, respectively, the values of $\overline{V}$, k, and q_{max}/c_m that were obtained with the two-pulse protocol (Figs. 5 *A* and 6 *A*). A single Boltzmann function plus a constant was least-squares fitted, with gap corrections, to the OFF charge at −90 mV vs. voltage data. The potential during the second pulse was −62 mV for fibers 127872 and 410871 and −60 mV for the other fibers; the duration of the second pulse was 120 ms for fiber 127872 and 100 ms for the other fibers. Columns 5–7 give the values of $\overline{V}$, k, and q_{max}/c_m that were obtained with the one-pulse protocol (from the second row in columns 5–7 in Table III in Hui and Chandler, 1990). These values were estimated from the Q_γ Boltzmann function that was obtained from a least-squares fit, with gap corrections, of a sum of two Boltzmann functions to charge vs. voltage data from a one-pulse experiment. Column 8 gives the values of $\Delta\overline{V}$, the difference between the values of $\overline{V}$ in columns 2 and 5. Column 9 gives the values of Δk, the difference between the values of k in columns 3 and 6. Column 10 gives the values of ρ, the ratio of the values of q_{max}/c_m in columns 4 and 7. Column 11 gives the values of τ_γ, the apparent time constant of I_γ. These were calculated on the assumption that, in a two-pulse experiment, the change in Q_γ that occurred during the second pulse (to −60 or −62 mV) followed an exponential time course with a time constant, τ_γ, that was independent of the voltage of the first pulse (see Eq. 3). On this assumption, the value of ρ in column 10 should be equal to $\exp(-t/\tau_\gamma)$, in which t is the duration of the second pulse, 100–120 ms. The values in column 11 were calculated from the values of $-t$ divided by the natural logarithm of the corresponding values of ρ in column 10. Fiber diameters, 88–103 μm.

In all five experiments listed in Table II, the half-widths of the OFF currents at −90 mV had a sigmoid voltage dependence similar to that shown in Fig. 6 *B*. On average, the value of $V_{1/2}$, referred to the average membrane potential in the central-pool region, was −57.5 mV. This is 1.7 mV more positive than the mean value of $\overline{V}$ in column 2 of Table II, but the difference, even when taken pairwise, is not significant.

OFF Charge vs. Voltage Curves in a One-Pulse Experiment

In Fig. 6 *A*, a two-pulse protocol was used to estimate the potential dependence of the steady-state distribution of Q_γ charge between resting and active states. A second method to estimate this potential dependence is to fit a sum of two Boltzmann functions to the charge vs. voltage data from a one-pulse experiment (Hui and Chandler, 1990). Fig. 5 *B* shows traces that are similar to those in Fig. 5 *A* except that a second voltage pulse was not used.

The filled circles in Fig. 7 *A* show the values of OFF charge at −90 mV plotted as a function of pulse potential. The open circles show the values of ON charge at potentials ≥ −40 mV. It was not possible to obtain reliable estimates of ON charge between −60 and −45 mV, because of the small amplitude and slow time course of I_γ. The values of the open and closed circles are similar, indicating approximate ON/OFF charge equality.

The uppermost curve in Fig. 7 *A* shows the least-squares fit, with gap corrections, of a sum of two Boltzmann functions (see Methods) to the charge vs. voltage data. Only the filled circles were used for the fit, which is good. The curves labeled Q_β and Q_γ show the individual contributions of each Boltzmann function, with gap corrections. For Q_β, $\overline{V}$ = −34.3 mV, k = 12.0 mV, and q_{max}/c_m = 10.6 nC/μF. For Q_γ, $\overline{V}$ = −56.5 mV, k = 2.3 mV, and q_{max}/c_m = 12.6 nC/μF. The values of $\overline{V}$ and k for Q_γ are similar to those obtained in Fig. 6 *A*, −57.2 and 1.4 mV, respectively.

At voltages between −60 and −50 mV, slow I_γ humps become apparent in the traces of ON charge movement (Fig. 5) and the steady-state Q_γ charge distribution changes from resting to active (Figs. 6 *A* and 7 *A*). These observations are consistent with the idea that the charge movement associated with the I_γ hump is the same as that associated with the Q_γ Boltzmann function (Hui and Chandler, 1990).

Fig. 7 *B* shows the voltage dependence, without gap corrections, of the individual Q_β and Q_γ Boltzmann functions, as well as their sum, that were used for the fit in Fig. 7 *A*. At voltages ≤ −70 mV, the Q_γ Boltzmann function is nearly zero and the $Q_\beta + Q_\gamma$ curve contains contributions mainly from Q_β. This stands in contrast to the situation in Fig. 7 *A*, where both the Q_β and Q_γ curves contain contributions from gap corrections, so that $Q_\beta + Q_\gamma$ contains significant contributions from both Q_β and Q_γ. Another difference between the Q_β and Q_γ curves in Fig. 7, *A* and *B*, is that, because of gap corrections, the values in Fig. 7 *A* for the strongest depolarizations are smaller than those in Fig. 7 *B*. These properties of gap corrections are described in Figs. 2–5 and Table I of Hui and Chandler (1990).

Charge vs. voltage data were obtained with the one-pulse protocol in the five fibers used for Table II. Data from each fiber were least-squares fitted with a sum of two Boltzmann functions. The values of $\overline{V}$, k, and q_{max}/c_m for the Q_γ Boltzmann function are given in columns 5–7 of Table II. Columns 8 and 9 give, respectively, the differences between the values of $\overline{V}$ ($\Delta\overline{V}$) and k (Δk) for Q_γ charge obtained with the two-pulse (columns 2 and 3) and one-pulse (columns 5 and 6) protocols. On average, the value of $\overline{V}$ obtained with the two-pulse protocol was 3.9 mV more negative (column 8) than that obtained with the one-pulse protocol; this value is not significantly different from zero. On the other hand, the average difference in the values of k, −2.1 mV (column 9), is significantly different from zero, although we are

reluctant to attach much significance to this difference until it is confirmed with additional experiments. Thus, the two-pulse and one-pulse protocols give similar values of $\overline{V}$ for the voltage dependence of the steady-state distribution of Q_γ charge between resting and active states. The values of k obtained with the two procedures may be somewhat different but are clearly smaller than those obtained for Q_β charge,

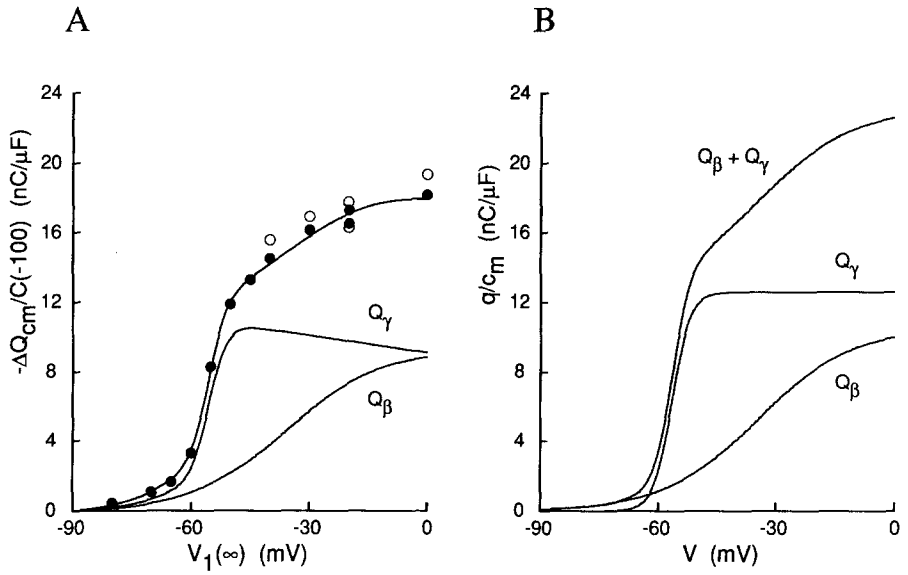

FIGURE 7. The charge vs. voltage curve measured after single depolarizing pulses, from the experiment in Fig. 5 *B*. (*A*) The filled circles show the values of OFF charge plotted, with reverse polarity, as a function of the pulse potential. The open circles show the values of ON charge for $V_1 \geq -40$ mV; these were determined with the procedure described in Hui and Chandler (1990). The continuous curve through the circles shows the least-squares fit, with gap corrections, of a sum of two Boltzmann functions (from columns 5–7 of Table III in Hui and Chandler, 1990); only the filled circles were used for the fit. The individual contributions of the Boltzmann functions are indicated by the curves labeled Q_β and Q_γ. For Q_β, $\overline{V} = -34.3$ mV, $k =$ 12.0 mV, and $q_{max}/c_m = 10.6$ nC/μF. For Q_γ, $\overline{V} = -56.5$ mV, $k = 2.3$ mV, and $q_{max}/c_m = 12.6$ nC/μF. The small progressive increases in the three theoretical curves between -90 and -65 mV arise from charge movement under the Vaseline seals (see Figs. 2–5 in Hui and Chandler, 1990). The negative slope in the Q_γ curve for $V_1 \geqq -45$ mV arises from the correction for the CONTROL pulse (see Figs. 2 *B* and 3 in Hui and Chandler, 1990). Time after saponin treatment of the end-pool segments, 49–74 min. (*B*) The Q_β and Q_γ Boltzmann functions that were used in *A*, and their sum, are plotted without gap corrections as a function of membrane potential.

on average 11.0 mV (SEM, 0.5 mV) (column 6 of Table III in Hui and Chandler, 1990).

The value of q_{max}/c_m obtained with the two-pulse protocol (Table II, column 4) is less than that obtained with the one-pulse protocol (Table II, column 7) because in a two-pulse experiment there is Q_γ charge movement during the second pulse. Column 10 in Table II gives the values of ρ (Eq. 3), the ratio of the values of q_{max}/c_m in columns

4 and 7. Although the time course of I_γ does not follow a simple exponential function at −90 mV (Fig. 9), and may not at −60 or −62 mV, it is of interest to calculate the apparent time constant τ_γ at −60 or −62 mV. Column 11 gives the values of τ_γ that were calculated from the equation $\rho = \exp(-t/\tau_\gamma)$, in which t is the duration of the second pulse. The mean value, 83 ms, lies within the range of values of τ_γ given in Table I, 88 ms in column 4 and 235 ms in column 6.

The Voltage Dependence of the Half-Width of the OFF Current in a One-Pulse Experiment

Fig. 8 shows the values of the half-width of the OFF current at −90 mV in the experiment illustrated in Fig. 5 *B*, plotted as a function of pulse potential. From −80

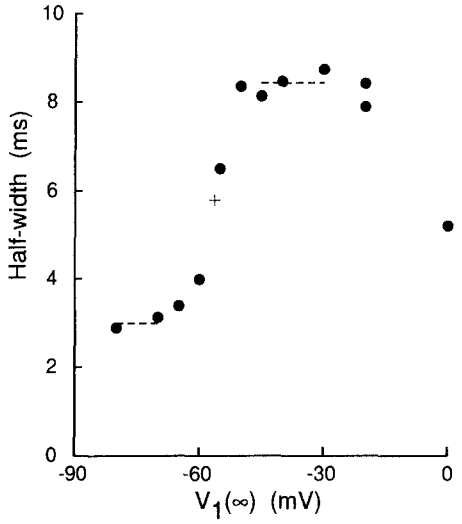

FIGURE 8. The voltage dependence of the half-width of the OFF charge movement measured after single depolarizing pulses, from the experiment in Fig. 5 *B*. The filled circles show the half-widths plotted as a function of the pulse potential. The lower horizontal dashed line shows the mean value of the half-width from −80 to −70 mV, 3.0 ms; the upper horizontal dashed line shows the mean value from −45 to −30 mV, 8.4 ms. The cross is plotted with the abscissa equal to $V_{1/2}$, −56.5 mV, and the ordinate equal to the average value of the two horizontal lines, 5.7 ms. The value of −56.5 mV in the voltage-measuring end pool corresponds to a value of −57.8 mV for the mean membrane potential in the central-pool region (based on a linear gradient of potential along the inside of the fiber and $r_e/(r_i + r_e) = 0.988$; Hui and Chandler, 1990). Time after saponin treatment of the end-pool segments, 49–74 min.

to −65 mV, the half-width was relatively constant at ~3 ms. From −65 to −50 mV it increased to 8–9 ms, and from −50 to −30 mV it showed little change. At potentials more positive than −30 mV, the half-width progressively decreased.

In Fig. 8, the value of $V_{1/2}$ was taken, somewhat arbitrarily, as the voltage at which the half-width is estimated by linear interpolation to be halfway between the mean values in the intervals −80 to −70 mV and −45 to −30 mV (3.0 and 8.4 ms, respectively, illustrated by dashed horizontal lines). A cross marks $V_{1/2}$, −56.5 mV, and its corresponding half-width, 5.7 ms. A value of −56.5 mV in the voltage-measuring end pool corresponds to a value of −57.8 mV for the mean membrane potential in the central-pool region (based on a linear gradient of potential along the inside of the fiber and $r_e/(r_i + r_e) = 0.988$; Chandler and Hui, 1990).

The value of $V_{1/2}$ obtained with the one-pulse protocol, −57.8 mV, is similar to that obtained with the two-pulse protocol, −54.9 mV. These values of potential refer to the mean membrane potential in the central-pool region and are taken from the estimates in Figs. 6 *B* and 8, respectively. In the five experiments listed in Table II, the mean value of $V_{1/2}$ associated with the one-pulse protocol was 0.9 mV more negative (SEM, 0.6 mV) than that associated with the two-pulse protocol; the difference is not significant, even when taken pairwise. Thus, with both the one-pulse and the two-pulse protocols, the same charge movement process, namely Q_γ, appears to underlie the abrupt increase in half-width of the OFF current at −90 mV that is observed when the potential of the first pulse is increased from −60 to −50 mV.

In Fig. 8, the voltage dependence of the OFF half-width at −90 mV can be explained qualitatively on the basis that I_γ has a broader time course than I_β and that I_β and I_γ make different relative contributions to the OFF charge movement after pulses to different potentials. The contributions of Q_β and Q_γ to the total amount of OFF charge, with gap corrections, are expected to be given by the theoretical curves in Fig. 7 *A*. The time course of the currents from OFF charge movement, however, may be distorted by contributions from currents under the Vaseline seals and by the waveform of the CONTROL current that was subtracted from the TEST current (Chandler and Hui, 1990; Hui and Chandler, 1990). Consequently, the Q_β and Q_γ curves in Fig. 7, *A* and *B*, are expected to provide only a qualitative understanding of the effect of pulse potential on OFF half-width. From −80 to −65 mV, the OFF half-width in Fig. 8 is approximately constant at ~3 ms. This is consistent either with the curves in Fig. 7 *A*, in which the contributions of both Q_β and Q_γ to the total charge increase but in relatively constant proportion, or with the curves in Fig. 7 *B*, in which Q_β accounts for almost all the total charge. From −60 to −50 mV, the half-width in Fig. 8 markedly increases. This is consistent with the curves in Fig. 7, *A* and *B*, in which the contribution of Q_γ to the total charge increases markedly whereas that of Q_β increases only slightly. From −50 to −30 mV the half-width in Fig. 8 is approximately constant, and from −20 to 0 mV it decreases. This is roughly consistent with the curves in Fig. 7, *A* and *B*, in which the relative contribution of Q_β to the total charge progressively increases.

In the five fibers listed in Table II, the voltage dependence of the OFF half-width at −90 mV had the same general features as those shown in Fig. 8. In two fibers, one of which was used for Fig. 8, the value of the half-width was relatively constant from −50 to −30 mV and then progressively decreased as the potential approached 0 mV. In the other three fibers, the half-width progressively decreased from −50 to 0 mV. In the five fibers, the mean half-width after a pulse to 0 mV was 0.69 (SEM, 0.03) times that after a pulse to −40 mV.

Estimate of the Time Course of I_γ *at −90 mV*

In Fig. 6 *B*, the half-width of the OFF charge movement at −90 mV was ~3 ms when the potential of the first pulse was between −90 and −65 mV and 7–9 ms when the potential was between −45 and 0 mV. Within each of these two voltage ranges, the individual charge movement traces practically superimposed (not shown). Fig. 9 *A* shows the average OFF charge movement when the potential of the first pulse was between −90 and −65 mV (trace *a*) and between −45 and 0 mV (trace *b*). Both the

peak value and half-width of trace *b* are larger than those of trace *a*. The half-widths of traces *a* and *b* are 3.2 and 8.1 ms, respectively.

Eq. 3 can be used to roughly estimate the contributions of Q_β and Q_γ charge to the charge movement currents in Fig. 9 *A*. Both traces contain a contribution from Q_β and Q_γ that is given by the first term (in brackets) on the right-hand side of Eq. 3. The traces also contain a contribution from Q_γ charge that is given by $\rho Q_\gamma(V)$. If the amount of Q_γ charge in the active state is given by the Boltzmann function used for Fig. 6 *A*, $Q_\gamma(V)$ is approximately equal to 0 after a pulse between −90 and −65 mV and is approximately equal to its maximal value after a pulse between −45 and 0 mV. If the value of ρ is independent of the potential of the first pulse, the difference between traces *b* and *a*, which is shown in Fig. 9 *B*, should contain a contribution from Q_γ but not from Q_β. According to this reasoning, the trace in Fig. 9 *B* is expected to

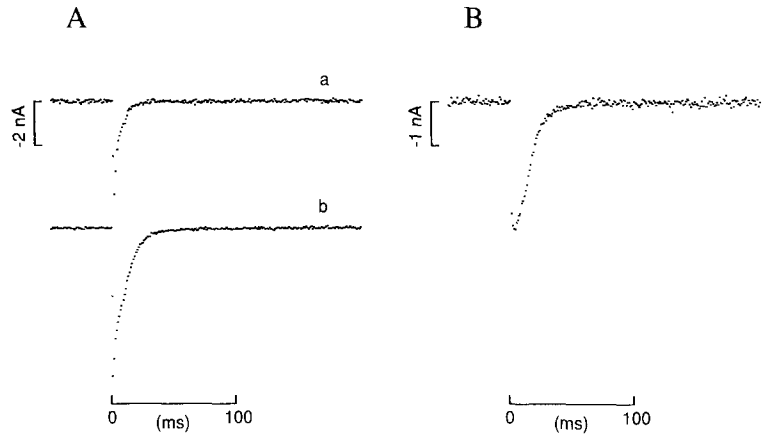

FIGURE 9. Time course of OFF charge movement at −90 mV obtained with the two-pulse protocol, from the experiment in Fig. 5 *A*. (*A*) The traces labeled *a* and *b* show the average currents obtained when the voltage of the first pulse was −90 to −65 mV (four measurements) and −45 to 0 mV (six measurements), respectively. (*B*) The trace represents the difference between traces *b* and *a* in *A*.

represent the temporal waveform of I_γ at −90 mV. This trace is less peaky than those in Fig. 9 *A*. Its time course is somewhat sigmoid and has a half-width of 15.3 ms. Similarly, the waveform of I_β is expected to be given by that of trace *a* in Fig. 9 *A* minus an unknown contribution from I_γ. This waveform is expected to be peaky and to have a half-width <3.2 ms, the half-width of trace *a* in Fig. 9 *A*.

As mentioned in the preceding section, the time course of any current recorded with the double Vaseline-gap method may be distorted by contributions from currents under the Vaseline seals and, in the case of intramembranous charge movement, from the CONTROL current. In Fig. 9 *A*, all the OFF currents that were used for traces *a* and *b* were obtained after a repolarization from −62 to −90 mV. Consequently, the variation of membrane potential along the fiber at the beginning of each OFF pulse is expected to have been similar for all the traces. For this reason,

the difference between traces *a* and *b* is likely to be due to a genuine difference in the time courses of the currents carried by intramembranous charge movement; that is, to a genuine difference in the time courses of the OFF I_β and I_γ. In addition, since the same factor was used to scale the CONTROL currents that were subtracted from the TEST currents in Fig. 9 *A*, the difference trace in Fig. 9 *B* does not contain a contribution from the CONTROL current. It therefore seems likely that the trace in Fig. 9 *B* represents a reasonable approximation to the actual waveform of the OFF I_γ at −90 mV.

Traces of OFF charge movement at −90 mV, similar to those in Fig. 9, were obtained in the five experiments listed in Table II. On average, the half-width of the OFF charge movement was 3.8 ms (SEM, 0.2 ms) when the potential of the first pulse was between −90 and −65 mV and 7.9 ms (SEM, 0.3 ms) when the potential was between −45 and 0 mV. The difference traces, which are expected to represent the time course of I_γ, were all somewhat sigmoid and had a mean half-width of 14.6 ms (SEM, 0.5 ms). Since the mean half-width of I_β is expected to be <3.8 ms, the ratio of the half-width of I_γ to that of I_β is expected to be $>14.6/3.8$ or >3.8, indicating that the time course of I_γ at −90 mV is considerably slower than that of I_β.

ON/OFF Charge Equality

Csernoch et al. (1989) reported that, under certain experimental conditions in which I_γ humps are present, the amount of ON Q_γ charge can exceed the amount of OFF Q_γ charge. We therefore attempted to estimate the amount of ON charge in an experiment in which a pronounced I_γ hump was visible in the ON TEST minus CONTROL current.

Fig. 10 *A* shows records from an experiment in which the duration of a pulse to −50 mV was varied from 10 to 200 ms. The upper set of records shows $V_1(t)$ and the lower set shows TEST minus CONTROL currents. These current records are similar to those in Fig. 1 *A* except that the ON current in Fig. 10 *A* has a pronounced I_γ hump that reached a peak value 20–30 ms after the start of the depolarization.

The filled circles in Fig. 10 *B* show the values of OFF charge plotted with reverse polarity as a function of pulse duration, from the experiment illustrated in Fig. 10 *A*. The curve represents a least-squares fit of an exponential function plus a constant; the initial and final values of the curve are 1.1 and 11.0 nC/μF, respectively, and the time constant of the exponential function is 31 ms. The finding that the curve provides a reasonable fit to the data may be somewhat surprising since the time course of the transient part of the ON current, from 10 to 200 ms, clearly deviates from that of a single decreasing exponential function (Fig. 10 *A*).

Fig. 11 *A* shows the voltage and current traces from the 200-ms pulse in Fig. 10 *A*. An exponential function plus a sloping straight line was least-squares fitted to the current in the interval between the vertical tick and the end of the trace. The sloping line from the fit, which is plotted, was used to estimate the ionic current during the depolarization. It was rounded by the voltage template and subtracted from the TEST minus CONTROL current to give the current carried by intramembranous charge movement (not shown) (Hui and Chandler, 1990).

Fig. 11 *B* shows the integral of the current carried by intramembranous charge movement, from Fig. 11 *A*, plotted as a function of the duration of the depolariza-

tion. The filled circles in Fig. 11 *C* show the values of the curve in Fig. 11 *B* at the times of repolarization used in Fig. 10. These points are fitted reasonably well by an exponential function plus a constant, as shown. The time constant of the exponential function, 26 ms, is similar to that obtained in Fig. 10 *B*, 31 ms.

In the experiment illustrated in Figs. 10 and 11, the amount of ON charge appears to be less than the amount of OFF charge. In Fig. 10 *B* the amount of OFF charge after a 200-ms depolarization was 11.0 nC/μF, whereas in Fig. 11 *C* the amount of ON charge after the same depolarization was 7.5 nC/μF. Thus, in this experiment the amount of ON charge that moved during a 200-ms depolarization to −50 mV

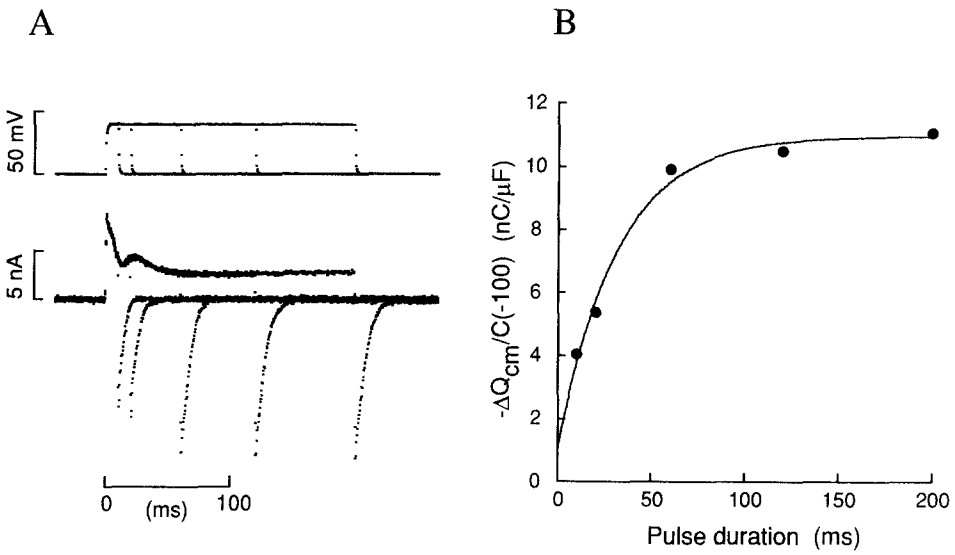

FIGURE 10. Time course of charge movement during a step depolarization to −50 mV. (*A*) The top set of superimposed traces shows $V_1(t)$ for 10-, 20-, 60-, 120-, and 200-ms depolarizations to −50 mV. The bottom set of traces shows the corresponding TEST minus CONTROL currents. (*B*) Filled circles, OFF charge measured after repolarization to −90 mV is plotted, with reverse polarity, as a function of pulse duration, from the experiment illustrated in *A*. The curve represents a best least-squares fit of the data with an exponential function plus a constant; it is given by [−9.9·exp (−*t*/31 ms) + 11.0] nC/μF. Fiber 407872; diameter, 98 μm; time after saponin treatment of the end-pool segments, 126–141 min.

appears to be 3.5 nC/μF less than the amount of OFF charge that moved after repolarization to −90 mV. This finding is different from that of Csernoch et al. (1989), in which the amount of ON charge sometimes exceeded the amount of OFF charge.

Since the estimates of ON charge in Fig. 11 depend on the slope and vertical position of the straight line that was used for the ionic current, shown in Fig. 11 *A*, it seemed important to find out whether a different line might give better agreement between the amounts of ON and OFF charge that are estimated with different pulse durations. Fig. 12 *A* shows the same voltage and current records as Fig. 11 *A*. The

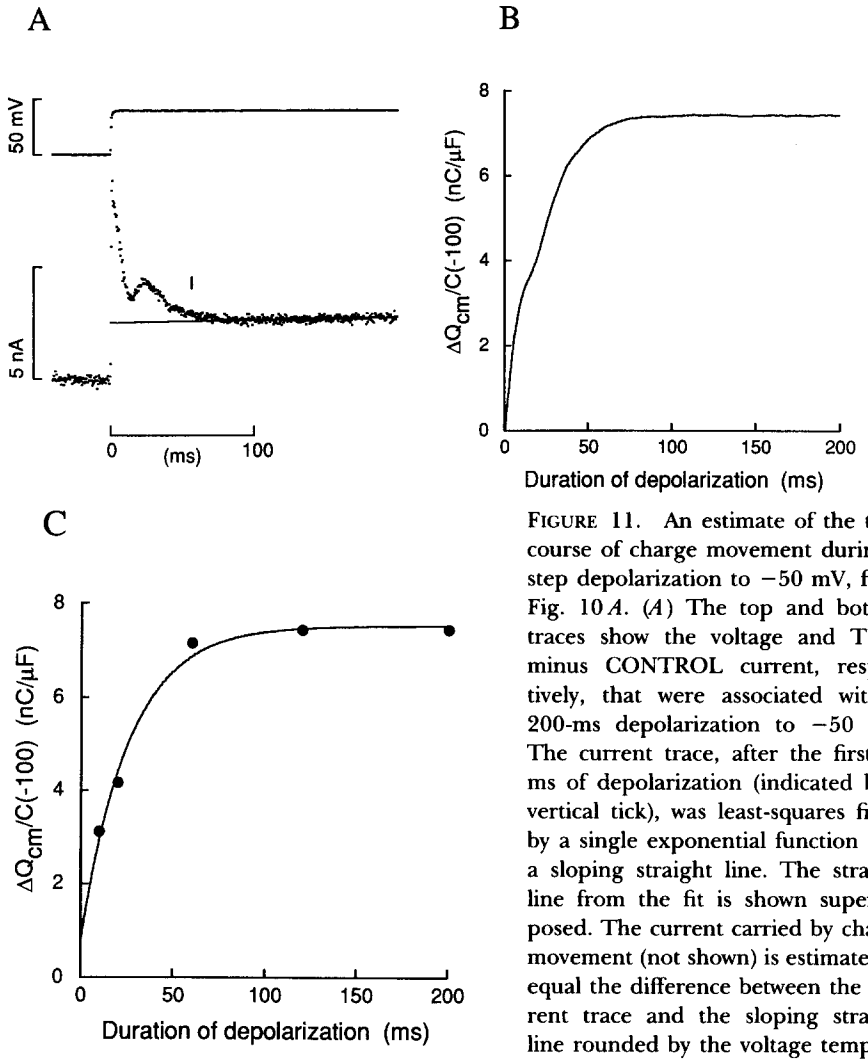

FIGURE 11. An estimate of the time course of charge movement during a step depolarization to −50 mV, from Fig. 10 *A*. (*A*) The top and bottom traces show the voltage and TEST minus CONTROL current, respectively, that were associated with a 200-ms depolarization to −50 mV. The current trace, after the first 56 ms of depolarization (indicated by a vertical tick), was least-squares fitted by a single exponential function plus a sloping straight line. The straight line from the fit is shown superimposed. The current carried by charge movement (not shown) is estimated to equal the difference between the current trace and the sloping straight line rounded by the voltage template (as described in Hui and Chandler, 1990). (*B*) The amount of ON charge, obtained by integration of the current carried by charge movement in *A* and normalized by $C(-100)$, is plotted as a function of the duration of the depolarization. (*C*) The filled circles represent the values of the curve in *B* at 10, 20, 60, 120, and 200 ms, the same durations used in Fig. 10. The curve represents a best least-squares fit of the points with an exponential function plus a constant; it is given by $[-6.8 \cdot \exp(-t/26 \text{ ms}) + 7.5]$ nC/μF.

slope and vertical position of the straight line were adjusted to minimize the ON/OFF charge inequality (i.e., to minimize the sum of the squared differences between the absolute values of the OFF charge from Fig. 10 *B* and the ON charge calculated for the same durations of depolarization). The continuous curve in Fig. 12 *B* shows the integral of the ON current carried by intramembranous charge movement, plotted as a function of the duration of the depolarization. The filled circles, which show the

values of OFF charge from Fig. 10 *B*, are in reasonable agreement with the values of ON charge.

Figs. 11 and 12 illustrate the difficulty involved in the estimation of the amount of ON charge at potentials where the kinetics of charge movement are slow. If the sloping straight line in Fig. 11 *A* is used to estimate ionic current, the amount of ON charge appears to be less than the amount of OFF charge. On the other hand, if the straight line in Fig. 12 *A* is used, there is approximate ON/OFF charge equality. Since both straight lines appear to provide reasonable estimates of the ionic current up to 200 ms, it would be necessary to use a current record considerably longer than 200 ms to reliably estimate the correction for ionic current in this example.

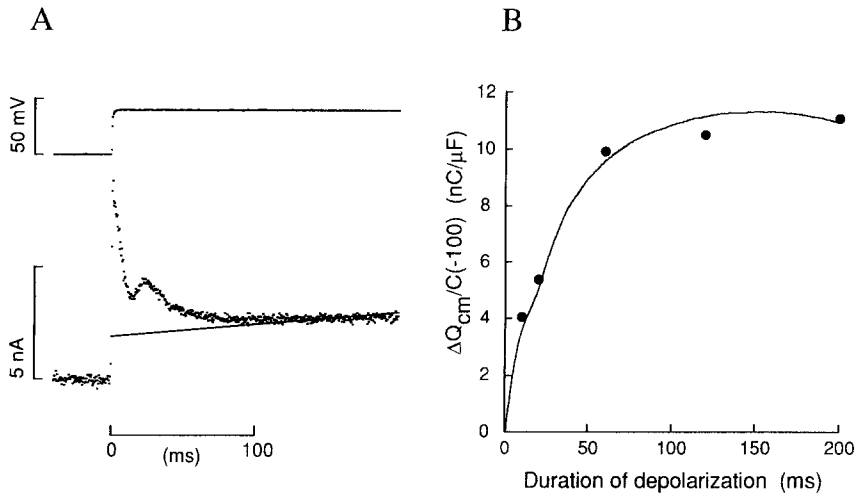

FIGURE 12. A second estimate of the time course of charge movement during a step depolarization to −50 mV, from Fig. 10 *A*. (*A*) The voltage and current traces are the same as those in Fig. 11 *A*. The vertical position and slope of the straight line have been adjusted to minimize the sum of the squared differences between the absolute values of the OFF charge from Fig. 10 *B* and the ON charge calculated for the same durations of depolarization. (*B*) The filled circles show the negative values of the OFF charge from Fig. 10 *B* and the continuous curve shows the ON charge from *A*.

DISCUSSION

The results described in this article provide new information about intramembranous charge movement in skeletal muscle and, in particular, about the slow time course of I_γ at potentials near −60 mV and about the voltage dependence of OFF charge at −90 mV obtained with a two-pulse protocol. In the next two sections, two simple models for the Q_β and Q_γ components of charge movement will be considered: a model in which Q_β and Q_γ represent the two transitions in a sequential three-state model of charge movement, and one in which they represent two separate species of intramembranous charge that can move in a parallel and independent manner.

Analysis of Charge vs. Voltage Data with a Sequential Three-State Model of Charge Movement

In a series of experiments on cut fibers, Melzer et al. (1986) measured intramembranous charge movement and myoplasmic Ca transients simultaneously. They were particularly interested in studying subthreshold and suprathreshold components of intramembranous charge movement. Although they were unable to distinguish or separate these two components kinetically, they were able to fit their steady-state charge vs. voltage data with a three-state, two-transition model of charge movement,

$$\mathrm{A} \overset{Q_1}{\longleftrightarrow} \mathrm{B} \overset{Q_2}{\longleftrightarrow} \mathrm{C}$$

At rest, most of the charge is in state A. After a strong depolarization, some of the charge can move from A to B and eventually to C, where it is assumed to be able to activate SR Ca permeability. Q_1 and Q_2 are used to denote the charge associated with the A–B and B–C transitions, respectively. Since only the Q_2 transition affects SR Ca permeability, Melzer et al. (1986) identified Q_1 with subthreshold charge and Q_2 with suprathreshold charge. They also suggested that Q_1 and Q_2 might correspond, respectively, to Q_β and Q_γ, since previous workers had suggested that Q_γ charge might play a role in the regulation of SR Ca release (Almers, 1978; Huang, 1982; Hui, 1983*b*; Vergara and Caputo, 1983).

In the sequential model, q_{max}, the amount of charge per unit length of fiber that would be associated with all the charge moving from state A to state C, is given by

$$q_{max} = q_{1,max} + q_{2,max} \tag{4}$$

in which $q_{1,max}$ and $q_{2,max}$ represent the contributions from Q_1 and Q_2, respectively. Since the same number of intramembranous particles is assumed to be associated with $q_{1,max}$ and $q_{2,max}$,

$$k_1 q_{1,max} = k_2 q_{2,max} \tag{5}$$

(Melzer et al., 1986). In the steady state, the distribution of charge between A and B or between B and C is assumed to obey a Boltzmann distribution function (Eq. 1).

Fig. 13*A* shows the OFF charge vs. voltage data that are shown in Fig. 7*A*. The theoretical curve represents a least-squares fit, with gap corrections, of the sequential three-state model. It provides a fit as good as that in Fig. 7*A*. The foot of the theoretical curve, from −90 to −65 mV, is similar to the one in Fig. 7*A*; its shape is determined mainly by the gap correction procedure. According to the fit, the Q_1 transition is more steeply voltage dependent than the Q_2 transition. The Boltzmann distribution function associated with Q_1 is determined by $\overline{V}_1 = -55.9$ mV and $k_1 =$ 3.3 mV and that associated with Q_2 by $\overline{V}_2 = -26.5$ mV and $k_2 = 7.7$ mV; $q_{max}/c_m =$ 22.4 nC/μF.

Fits similar to the one in Fig. 13*A*, with gap corrections, were made with the same charge vs. voltage data that were used for Table III in Hui and Chandler (1990). Columns 2–6 of Table III in this article give the values of the fitted parameters. On average, $\overline{V}_1 = -55.9$ mV, $k_1 = 3.7$ mV, $\overline{V}_2 = -27.4$ mV, $k_2 = 8.2$ mV, and $q_{max}/c_m =$ 23.2 nC/μF. In every fiber, $k_1 < k_2$; on average, $k_1/k_2 = 0.46$ (column 7). Thus, the properties of the Q_1 charge transition are those that are normally associated with Q_γ:

a steep voltage dependence that occurs at potentials where slow I_γ humps first become apparent, between −60 and −50 mV in our experiments. By elimination, the Q_2 transition is expected to be associated with Q_β.

The charge vs. voltage data that were used for Table III were well fitted with either the sequential three-state model or a sum of two Boltzmann functions. Column 8 of Table III gives the values of the residual sum of squares for the fits with the sequential model and column 7 of Table IV in Hui and Chandler (1990) gives the corresponding values for the fits with a sum of two Boltzmann functions. In two fibers (120871 and 127872), the sequential model gave a better fit. In the other eight fibers, a sum of two Boltzmann functions gave a better fit. Thus, on average, a sum of two

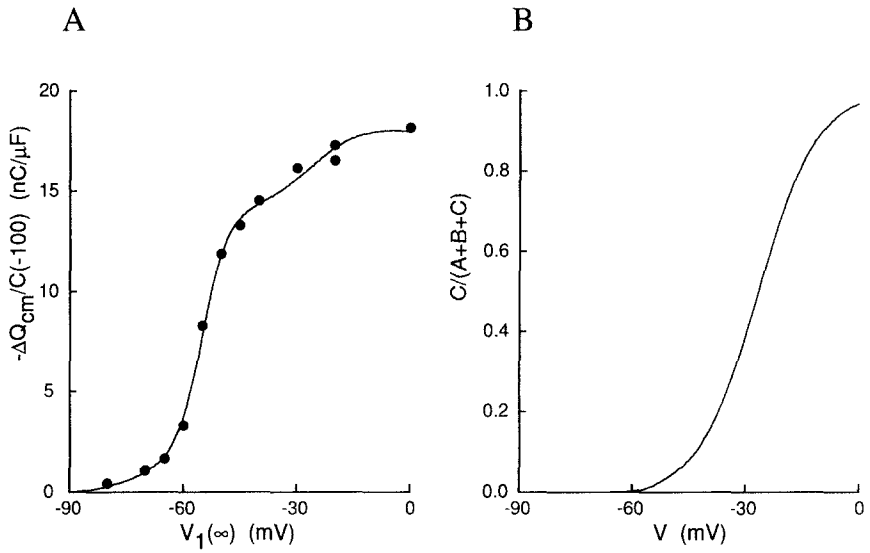

FIGURE 13. Use of a three-state, two-transition model of charge movement to fit charge vs. voltage data. (*A*) The filled circles show the same data as Fig. 7 *A*. The curve represents the best least-squares fit, with gap corrections, of the sequential three-state model described in Melzer et al. (1986) and in the Discussion section of this article, with $\overline{V}_1$ = −55.9 mV, k_1 = 3.3 mV, $\overline{V}_2$ = −26.5 mV, k_2 = 7.7 mV, and q_{max}/c_m = 22.4 nC/μF. (*B*) The curve shows the steady-state fractional occupancy of state C, without gap corrections, plotted against voltage. From the fit in *A*.

Boltzmann functions gave a somewhat better fit than the sequential three-state model. This is to be expected because the two Boltzmann function model has six degrees of freedom, whereas the sequential model has only five degrees of freedom.

Since Melzer et al. (1986) did not use gap corrections in the least-squares fits of their charge vs. voltage data, we also fitted our data with the sequential three-state model without gap corrections. The mean values of the adjustable parameters were $\overline{V}_1$ = −56.6 mV (SEM, 1.1 mV), k_1 = 4.3 mV (SEM, 0.3 mV), $\overline{V}_2$ = −35.9 mV (SEM, 2.2 mV), k_2 = 8.7 mV (SEM, 0.5 mV), and q_{max}/c_m = 18.7 nC/μF (SEM, 1.2 nC/μF). The value of k_1 was always smaller than that of k_2 and, on average, k_1/k_2 = 0.50 (SEM, 0.03). These values are similar to those obtained with gap corrections (Table III)

except that the mean value of q_{max}/c_m without gap corrections is only ~0.8 times that with gap corrections (similar to the findings in Tables I and II in Hui and Chandler, 1990).

Some of the experimental results obtained by Melzer et al. (1986) were somewhat different from those obtained by us. I_γ humps were not apparent in their records of ON charge movement and their charge vs. voltage data were not as steeply voltage dependent as ours. When fitted with a single Boltzmann function, without gap

TABLE III

Parameters from Charge vs. Voltage Data Fitted with a Three-State, Two-Transition Model of Charge Movement

(1) Fiber reference	(2) $\overline{V}_1$	(3) k_1	(4) $\overline{V}_2$	(5) k_2	(6) q_{max}/c_m	(7) k_1/k_2	(8) Residual sum of squares	(9) V_C
	mV	*mV*	*mV*	*mV*	*nC/μF*		*(nC/μF)²*	*mV*
120871	−52.3	4.3	−25.6	10.1	14.0	0.43	0.469	5.4
127872	−51.9	4.8	−16.3	12.9	27.4	0.37	3.796	6.9
331871	−54.0	3.2	−24.2	7.5	22.2	0.43	0.081	6.1
401872	−57.5	2.6	−32.0	5.4	21.6	0.48	4.304	5.1
406871	−57.2	2.1	−34.9	4.7	19.9	0.45	2.643	4.4
407871	−58.4	4.2	−30.7	8.0	21.5	0.53	3.160	5.8
407872	−64.4	4.2	−37.5	8.2	26.5	0.51	3.543	5.8
409871	−52.2	4.8	−20.0	9.5	28.4	0.51	4.743	6.6
409872	−55.4	3.2	−26.4	7.5	28.2	0.43	4.910	6.0
410871	−55.9	3.3	−26.5	7.7	22.4	0.43	1.346	6.0
Mean	−55.9	3.7	−27.4	8.2	23.2	0.46		5.8
SEM	1.2	0.3	2.1	0.7	1.4	0.02		0.2

Column 1 gives the fiber references. The charge vs. voltage data that were used for Table III in Hui and Chandler (1990) were least-squares fitted, with gap corrections, with the predictions of the three-state, two-transition model of Melzer et al. (1986) (see Discussion). The steady-state distributions of charge between states A and B and between B and C were assumed to obey Boltzmann distribution functions; i.e., each of the steady-state ratios B/(A + B) and C/(B + C) was assumed to be given by an equation similar to Eq. 1. Subscripts 1 and 2 are used to denote the parameters associated with the A–B and B–C transitions, respectively. Columns 2–6 give, respectively, the values of $\overline{V}_1$, k_1, $\overline{V}_2$, k_2, and q_{max}/c_m that were obtained from the fits. Column 7 gives the values of k_1/k_2. Column 8 gives the values of the residual sum of squares of the fits, which can be compared with the values in column 7 of Table IV in Hui and Chandler (1990). Column 9 gives the values of V_C, the *e*-fold factor for the increase in the steady-state fractional occupancy of state C with voltage near the mechanical threshold. The function $A \cdot \exp(V/V_C)$ was least-squares fitted to the steady-state values of C/(A + B + C) at 1-mV intervals from $V = -70$ mV to the first voltage that gave a value of C/(A + B + C) that exceeded 0.1.

corrections, their charge vs. voltage data gave a mean value of 21.5 mV for k, whereas our data, fitted with the same procedure, gave 6.3 mV (column 3 of Table II in Hui and Chandler, 1990). When fitted with the sequential three-state model, also without gap corrections, the data of Melzer et al. (1986) gave mean values of 12.3 and 12.9 mV for k_1 and k_2, respectively, whereas our data gave 4.3 and 8.7 mV, respectively (preceding paragraph).

Some of these differences may be attributed to the use by Melzer et al. (1986) of a SO_4-containing solution in the central pool and our use of a Cl-containing solution. In our experiments, replacement of Cl with SO_4 increased the mean value of k, estimated from fits with a single Boltzmann function without gap corrections, from 6.3 mV (column 3 of Table II in Hui and Chandler, 1990) to 10.5 mV (column 6 of Table V in Hui and Chandler, 1990). The reason for the remaining difference, between our value of 10.5 mV in a SO_4 solution and Melzer et al.'s value of 21.5 mV, is not known but may be related to other differences in the experimental conditions. For example, cold-adapted *Rana temporaria* were used in our experiments, whereas room temperature–adapted *Rana pipiens* were used in Melzer et al.'s experiments. We used 20 mM creatine phosphate and 20 mM EGTA in the internal solution, whereas they used no creatine phosphate and only 0.1 mM EGTA. Our experiments were carried out at 13–14°C, whereas theirs were carried out at 5–10°C. Both sets of experiments were carried out on fibers stretched to about the same degree: our fibers had a striation spacing of 3.5–3.6 μm, whereas their fibers were "stretched to sarcomere lengths allowing little or no overlap of thick and thin contractile filaments."

Although the sequential three-state model provides a good fit to our charge vs. voltage data (Fig. 13 *A* and Table III) and is attractive in many ways, it fails to explain four important properties of charge movement and its relation to SR Ca release, as described below.

The voltage dependence of SR Ca release. Near the mechanical threshold, SR Ca release increases *e*-fold every 2–4 mV. This has been shown in intact fibers (Baylor et al., 1979, 1983; Miledi et al., 1981) and in cut fibers that contain 0.1 mM EGTA (Maylie et al., 1987*a*, *b*). Such a steep voltage dependence is not predicted by the sequential three-state model of Melzer et al. (1986), at least in its original form. Fig. 13 *B* shows the steady-state fractional occupancy of state C, given by C/(A + B + C), plotted as a function of voltage, without gap corrections. According to the assumption used by Melzer et al. (1986), C/(A + B + C) gives the degree of activation of SR Ca permeability. The foot of the curve, from −70 mV to the first voltage at which C/(A + B + C) > 0.1, was least-squares fitted with the function A·exp (V/V_C). The fit was good (not shown) and the value of V_C was 6.0 mV. Column 9 of Table III gives the values of V_C from this and nine other experiments. The mean value is 5.8 mV (SEM, 0.2 mV), which is significantly larger than the value of 4 mV, the upper range of the *e*-fold factor for SR Ca release. Thus, the sequential three-state model fails to account for the steepness of the voltage dependence of SR Ca release near the mechanical threshold, a deficiency also noted by Melzer et al. (1986) in their experiments.

The time course of intramembranous charge movement near −60 mV. When the voltage is stepped from the holding potential of −90 to −60 mV, the time course of intramembranous charge movement has an early rapid outward component followed by a delayed outward component (Fig. 1). Since almost all the charge is expected to be in state A at the holding potential (as determined from the values of $\overline{V}$ and k in columns 2–5 in Table III), this finding requires the Q_1 transition to be rapid and the Q_2 transition to be slow. On the other hand, as discussed above, the voltage dependence of the Q_1 transition is steeper than that of Q_2 (Table III) so that Q_1 has been identified with Q_γ and Q_2 with Q_β. This implies that Q_γ is rapid and Q_β is slow,

contrary to the findings of Adrian and Peres (1977, 1979), Huang (1982), Hui (1983*a*, *b*), and this article, which indicate that, near −60 mV, the Q_β transition is rapid and the Q_γ transition is slow.

The shape of the OFF charge at −90 mV vs. voltage curve from a two-pulse experiment. According to the sequential three-state model, after a strong depolarization from the holding potential, some of the charge that is in state A should move to B and then to C. In a two-pulse experiment, such as that used for Fig. 6 *A*, when the voltage is stepped from that of the first pulse to that of the second pulse, −62 mV, most of the charge in C would tend to move to B and most of the charge in B would tend to move to A, according to the values $\overline{V}_1 = -55.9$ mV, $k_1 = 3.3$ mV, $\overline{V}_2 = -26.5$ mV, and $k_2 = 7.7$ mV that were obtained from the fit in Fig. 13 *A*. As discussed above, the Q_1 transition at −62 mV is expected to be fast and the Q_2 transition is expected to be slow. Consequently, the amount of charge in state B at the end of the second pulse is expected to be small and to approximately satisfy the steady-state distribution of charge between states A and B. The amount of charge in state C is expected to be equal to a fraction of the amount that was present at the beginning of the second pulse (or end of the first pulse).

After repolarization to −90 mV, the OFF charge contains contributions from the amounts of charge that were in states B and C at the end of the second pulse. According to the reasoning outlined in the preceding paragraph, the amount of charge that was in state C at the end of the second pulse is expected to be proportional to the amount of charge that was in state C at the end of the first pulse. The amount of charge that was in state B at the end of the second pulse is expected to be small and relatively independent of the potential of the first pulse, since a large fraction of the charge is expected to be in either state A or B at the end of the second pulse and to be in an approximately steady-state distribution. As a result, the charge vs. voltage relation in Fig. 6 *A* is expected to have approximately the same shape as the C/(A + B + C) vs. voltage curve in Fig. 13 *B* plus a small offset.

Preliminary numerical calculations verify the prediction that the charge vs. voltage relation in Fig. 6 *A* should have approximately the same shape as the C/(A + B + C) vs. voltage curve in Fig. 13 *B* plus an offset. The predicted relation is clearly different from that shown by the data in Fig. 6 *A*. The data show an abrupt increase from −60 to −50 mV, a plateau from −50 to −30 mV, and a gradual increase from −30 to 0 mV. On the other hand, the C/(A + B + C) vs. voltage curve in Fig. 13 *B* shows little change from −60 to −50 mV and then progressively increases as the voltage is increased to 0 mV. These differences are also present after the curve in Fig. 13 *B* is modified for gap corrections (not shown), as should be done for an exact comparison with the charge vs. voltage data in Fig. 6 *A*.

The voltage dependence of membrane capacitance at potentials between the holding potential and the mechanical threshold. Because of charge movement, the value of membrane capacitance increases as the potential is increased from the holding potential to a potential near the mechanical threshold. This has been observed in intact fibers (Adrian and Almers, 1976*a*; Schneider and Chandler, 1976) and may occur in cut fibers, although the double Vaseline-gap technique cannot reliably resolve small changes in capacitance near the holding potential (Fig. 14 in Hui and Chandler, 1990; also, see the foot of the theoretical curve through the experimental

points in Fig. 7 *A*). According to Schneider and Chandler (1976), this increase in intact fibers is approximately exponential with a mean *e*-fold factor of 12 mV. On the other hand, the sequential three-state model for charge movement predicts a mean *e*-fold factor of 3.7 mV, given by the mean value of k_1 in column 3 of Table III.

Analysis of Charge vs. Voltage Data with a Parallel Model of Charge Movement

The properties of intramembranous charge movement described in this article, including the four properties listed in the preceding section, are consistent with the idea that the Q_β and Q_γ components of intramembranous charge movement arise from two species of charge that can move in a parallel and independent manner (Adrian and Huang, 1984; Huang, 1986; Huang and Peachey, 1989), at least during a voltage-clamp step that lasts no longer than a few hundred milliseconds. In the simplest case, each species of charge is assumed to be distributed between a resting and an active state, and the steady-state distribution of each species is determined by a Boltzmann distribution function (Fig. 7 *A*). The Boltzmann functions for Q_β and Q_γ are different and, under many conditions, the time courses of I_γ and I_β are different. I_γ is slower than I_β during depolarizations from the holding potential to a voltage that is near or just past the mechanical threshold (Adrian and Peres, 1977, 1979; Huang, 1982; Hui, 1983*a*, *b*; Figs. 1 and 10 *A* in this article). It is also slower in a two-pulse experiment when the voltage is stepped from −40 to −60 mV (Figs. 3 and 4 *A*) or from −60 to −90 mV (Fig. 9). The parallel model is consistent with all these findings and, as shown below, with the four properties of charge movement and its relation to SR Ca release that were shown in the preceding section to be inconsistent with the sequential three-state model.

The voltage dependence of SR Ca release. As mentioned in the preceding section, SR Ca release is steeply voltage dependent near the mechanical threshold, with an *e*-fold increase for each additional 2–4 mV depolarization. Several investigators have suggested that the Q_γ component of charge might play a role in the regulation of Ca release from the SR into the myoplasm (Almers, 1978; Huang, 1982; Hui, 1983*b*; Vergara and Caputo, 1983). If the SR Ca permeability is directly proportional to the amount of Q_γ charge that is in the active state, the *e*-fold factor for SR Ca release near the mechanical threshold is given simply by the value of k for the Q_γ Boltzmann function. The average values of k in columns 3 and 6 of Table II are 1.2 and 3.3 mV, respectively, consistent with the idea that Q_γ charge plays a role in the regulation of SR Ca release.

Chandler et al. (1976) estimated the density of intramembranous charge groups from q_{max}/c_m = 25 nC/μF, k = 8 mV, and a value of 0.9 μF/cm^2 for the capacitance of the plasma membrane. The value they obtained, 500–600 groups per μm^2 referred to the area of the tubular membrane, is similar to the density of feet observed in frog muscle with the electron microscope (Franzini-Armstrong, 1970). The estimated number of charge groups decreases by a factor of 4–11 if the parameters associated with Q_γ are used, q_{max}/c_m = 15.1 nC/μF and k = 1.2–3.3 mV (Table II). If this estimate is correct, it indicates that the density of charge groups is only 0.1–0.3 times the density of feet. On the other hand, the actual density of charge groups would be larger than this estimate if there were positive cooperativity between neighboring charge groups.

The time course of intramembranous charge movement near −60 mV. The parallel model is clearly consistent with the idea that Q_β charge can move much more rapidly than Q_γ charge at voltages near −60 mV.

The shape of the OFF charge at −90 mV vs. voltage curve from a two-pulse experiment. The parallel model is consistent with the relation between OFF charge at −90 mV and voltage that is obtained with the two-pulse protocol (Fig. 6 *A*). At the end of the second pulse, Q_β charge but not Q_γ is expected to be in an approximately steady-state distribution. According to Eq. 3, if ρ is constant, the OFF charge vs. voltage relation should be given by $Q_\gamma(V)$, scaled by ρ, plus a constant offset. The fitted curve in Fig. 6 *A* was calculated in this manner with a Boltzmann distribution function for $Q_\gamma(V)$. The curve provides a good fit to the filled circles. The deviation of the open circles from the curve is discussed below.

The voltage dependence of membrane capacitance at potentials between the holding potential and the mechanical threshold. As illustrated in Fig. 7 *B*, there is little rearrangement of Q_γ charge when the voltage is changed from −90 to −65 mV. Consequently, in this range of potentials, the voltage dependence of membrane capacitance, without gap corrections, is due to Q_β. The value of the *e*-fold factor for capacitance reported by Schneider and Chandler (1976), 12 mV, is close to 11 mV, the average value of *k* for the Q_β Boltzmann function in our experiments (column 6 of Table III in Hui and Chandler, 1990).

All the results in this article appear to be consistent with the idea that Q_β and Q_γ represent two separate species of intramembranous charge that can move in a parallel and independent manner. To a first approximation, the steady-state distributions of Q_β and Q_γ each obey a Boltzmann distribution function. Only one result is not obviously consistent with this idea: in the two-pulse experiment, the OFF charge vs. voltage data deviate from the Boltzmann curve at strong depolarizations (open circles in Fig. 6 *A*). A deviation of this type was found in all five experiments with the two-pulse protocol and became apparent when the potential of the first pulse became more positive than a value between −40 and −20 mV (the exact potential depended on the fiber).

Four possible explanations for this deviation are given below. All four are consistent with the idea that Q_β and Q_γ move in a parallel and independent fashion, and all but the last one are consistent with the idea that the steady-state distribution of each component of charge approximately satisfies a Boltzmann distribution function. The first possibility is that the record of OFF charge is contaminated by ionic current when the potential of the first pulse is more positive than −40 to −20 mV. A second possibility is that the kinetics of Q_γ movement during the second pulse depend on the voltage of the first pulse. If the potential of the first pulse is made more positive than −40 to −20 mV, the rate at which Q_γ is able to move during the second pulse (to −60 or −62 mV) may decrease and the value of ρ in Eq. 3 may increase (the scatter of data in Fig. 4 *B* may be too great to resolve such an effect). A third possibility is that the kinetics of Q_β movement during the second pulse depend on the voltage of the first pulse. If the voltage of the first pulse is made more positive than −40 to −20 mV, the rate at which Q_β is able to move during the second pulse may become sufficiently slow that the OFF charge contains a significant contribution from Q_β. A fourth possibility is that the charge vs. voltage relation for Q_γ does not

obey a simple Boltzmann function between −90 and 0 mV, although it appears to obey such a function between −90 mV and −40 to −20 mV.

Conclusion

As described above, the simplest interpretation of our results is that, at least during a voltage-clamp step that lasts no longer than a few hundred milliseconds, Q_β and Q_γ represent different species of charge that appear to be able to move independently and in parallel, as suggested by Adrian and Huang (1984), Huang (1986), and Huang and Peachey (1989). To a first approximation, the results fit with the idea that each species can exist in a resting or an active state, and that the steady-state distribution is governed, at least at voltages between −90 mV and −40 to −20 mV, by a Boltzmann distribution function. If Q_β and Q_γ indeed represent different species of charge, it seems likely that the Q_γ component plays a role in the regulation of SR Ca release because its steady-state distribution is steeply voltage dependent near the mechanical threshold. For this reason, it is tempting to speculate that Q_γ is the component of charge movement that is associated with the transverse tubular dihydropyridine receptor (Rios and Brum, 1987; Tanabe et al., 1988; Adams et al., 1990). Q_β may also be associated with the dihydropyridine receptor (cf. page 291 of Hui and Chandler, 1990) or with a different molecule that remains to be identified. It is also possible that intramembranous charge movement contains more than two components.

Although our results appear to be consistent with the idea that Q_β and Q_γ represent different species of charge, they do not prove it. Thus, although the simple sequential three-state, two-transition model proposed by Melzer et al. (1986) can be ruled out, other models that link or couple Q_β and Q_γ may well work and should be explored. One interesting possibility is the one proposed by Csernoch et al. (1989) in which I_γ is caused by a shift in the charge vs. voltage curve that is produced by SR Ca release. In the evaluation of this and other models, it seems clear that any successful candidate will need to explain the results described in this article and, in particular, the four properties of charge movement that were used to rule out the sequential three-state model.

We thank the staff of the Electronics Laboratory in the Department of Cellular and Molecular Physiology of the Yale University School of Medicine for help with the design and construction of equipment. We also thank Steve Baylor, De-Shien Jong, Paul Pape, and Martin Schneider for helpful comments on the manuscript.

This work was supported by the U.S. Public Health Service (grant AM-37643 to W. K. Chandler, grant NS-21955 to C. S. Hui, and Research Career Development Award NS-00976 to C. S. Hui) and by the Muscular Dystrophy Association (C. S. Hui).

Original version received 19 June 1990 and accepted version received 30 March 1991.

REFERENCES

Adams, B. A., T. Tanabe, A. Mikami, S. Numa, and K. G. Beam. 1990. Intramembrane charge movement restored in dysgenic skeletal muscle by injection of dihydropyridine receptor cDNAs. *Nature.* 346:569–572.

Adrian, R. H., and W. Almers. 1976*a*. The voltage dependence of membrane capacity. *Journal of Physiology*. 254:317–338.

Adrian, R. H., and W. Almers. 1976*b*. Charge movement in the membrane of striated muscle. *Journal of Physiology*. 254:339–360.

Adrian, R. H., and C. L.-H. Huang. 1984. Experimental analysis of the relationship between charge components in skeletal muscle of Rana temporaria. *Journal of Physiology*. 353:419–434.

Adrian, R. H., and A. Peres. 1977. A 'gating' signal for the potassium channel? *Nature*. 267:800–804.

Adrian, R. H., and A. Peres. 1979. Charge movement and membrane capacity in frog muscle. *Journal of Physiology*. 289:83–97.

Almers, W. 1978. Gating currents and charge movements in excitable membranes. *Review of Physiological and Biochemical Pharmacology*. 82:96–190.

Baylor, S. M., W. K. Chandler, and M. W. Marshall. 1979. Arsenazo III signals in singly dissected frog twitch fibres. *Journal of Physiology*. 287:23–24P.

Baylor, S. M., W. K. Chandler, and M. W. Marshall. 1983. Sarcoplasmic reticulum calcium release in frog skeletal muscle fibres estimated from arsenazo III calcium transients. *Journal of Physiology*. 344:625–666.

Chandler, W. K., and C. S. Hui. 1990. Membrane capacitance in frog cut twitch fibers mounted in a double Vaseline-gap chamber. *Journal of General Physiology*. 96:225–256.

Chandler, W. K., R. F. Rakowski, and M. F. Schneider. 1976. Effects of glycerol treatment and maintained depolarization on charge movement in skeletal muscle. *Journal of Physiology*. 254:285–316.

Csernoch, L., I. Uribe, M. Rodriguez, G. Pizarro, and E. Rios. 1989. Qgamma and Ca release flux in skeletal muscle fibers. *Biophysical Journal*. 55:88*a*. (Abstr.)

Franzini-Armstrong, C. 1970. Studies of the triad. I. Structure of the junction in frog twitch fibers. *Journal of Cell Biology*. 47:488–499.

Hodgkin, A. L., and P. Horowicz. 1959. The influence of potassium and chloride ions on the membrane potential of single muscle fibres. *Journal of Physiology*. 148:127–160.

Hodgkin, A. L., and P. Horowicz. 1960. Potassium contractures in single muscle fibres. *Journal of Physiology*. 153:386–403.

Horowicz, P., and M. F. Schneider. 1981*a*. Membrane charge movement in contracting and non-contracting skeletal muscle fibres. *Journal of Physiology*. 314:565–593.

Horowicz, P., and M. F. Schneider. 1981*b*. Membrane charge moved at contraction thresholds in skeletal muscle fibres. *Journal of Physiology*. 314:595–633.

Huang, C. L.-H. 1982. Pharmacological separation of charge movement components in frog skeletal muscle. *Journal of Physiology*. 324:375–387.

Huang, C. L.-H. 1984. Analysis of 'off' tails of intramembrane charge movements in skeletal muscle of Rana temporaria. *Journal of Physiology*. 356:375–390.

Huang, C. L.-H. 1986. The differential effects of twitch potentiators on charge movements in frog skeletal muscle. *Journal of Physiology*. 380:17–33.

Huang, C. L.-H., and L. D. Peachey. 1989. Anatomical distribution of voltage-dependent membrane capacitance in frog skeletal muscle fibers. *Journal of General Physiology*. 93:565–584.

Hui, C. S. 1983*a*. Pharmacological studies of charge movement in frog skeletal muscle. *Journal of Physiology*. 337:509–529.

Hui, C. S. 1983*b*. Differential properties of two charge components in frog skeletal muscle. *Journal of Physiology*. 337:531–552.

Hui, C. S., and W. K. Chandler. 1988. Currents associated with intramembranous charge movement in frog cut twitch fibers. *Biophysical Journal*. 53:646*a*. (Abstr.)

Hui, C. S., and W. K. Chandler. 1990. Intramembranous charge movement in frog cut twitch fibers mounted in a double Vaseline-gap chamber. *Journal of General Physiology.* 96:257–297.

Hutter, O. F., and D. Noble. 1960. The chloride conductance of frog skeletal muscle. *Journal of Physiology.* 151:89–102.

Maylie, J., M. Irving, N. L. Sizto, and W. K. Chandler. 1987*a*. Comparison of arsenazo III optical signals in intact and cut frog twitch fibers. *Journal of General Physiology.* 89:41–81.

Maylie, J., M. Irving, N. L. Sizto, and W. K. Chandler. 1987*b*. Calcium signals recorded from cut frog twitch fibers containing antipyrylazo III. *Journal of General Physiology.* 89:83–143.

Melzer, W., M. F. Schneider, B. J. Simon, and G. Szucs. 1986. Intramembrane charge movement and calcium release in frog skeletal muscle. *Journal of Physiology.* 373:481–511.

Miledi, R., S. Nakajima, I. Parker, and T. Takahashi. 1981. Effects of membrane polarization on sarcoplasmic calcium release in skeletal muscle. *Proceedings of the Royal Society of London, Series B.* 213:1–13.

Rios, E., and G. Brum. 1987. Involvement of dihydropyridine receptors in excitation-contraction coupling in skeletal muscle. *Nature.* 325:717–720.

Schneider, M. F., and W. K. Chandler. 1973. Voltage dependent charge movement in skeletal muscle: a possible step in excitation-contraction coupling. *Nature.* 242:244–246.

Schneider, M. F., and W. K. Chandler. 1976. Effects of membrane potential on the capacitance of skeletal muscle fibers. *Journal of General Physiology.* 67:125–163.

Tanabe, T., K. G. Beam, J. A. Powell, and S. Numa. 1988. Restoration of excitation-contraction coupling and slow calcium current in dysgenic muscle by dihydropyridine receptor complementary DNA. *Nature.* 336:134–139.

Vergara, J., and C. Caputo. 1983. Effects of tetracaine on charge movements and calcium signals in frog skeletal muscle fibres. *Proceedings of the National Academy of Sciences, USA.* 80:1477–1481.